SCI. MAR., 61 (Supl. 1): 205-228 SCIENTIA MARINA 1997

LECTURES ON PLANKTON AND TURBULENCE. *C. MARRASÉ, E. SAIZ and J.M. REDONDO (eds.)*

Turbulence generation and measurement: application to studies on plankton*

FRANCESC PETERS[1] and JOSÉ M. REDONDO[2]

[1] Institut de Ciències del Mar (CSIC), Pg. Joan de Borbó, E-08039 Barcelona, Catalunya, Spain. E-mail: cesc@icm.csic.es.
[2] Departament de Física Aplicada, Universitat Politècnica de Catalunya, B5 Campus Nord, E-08034 Barcelona, Catalunya, Spain. E-mail: redondo@etseccpb.upc.es.

SUMMARY: Interest in the effects of small-scale turbulence on aquatic organisms has increased tremendously in recent years. Since the complete understanding of turbulence is still one of the last frontiers in physics, a study of its effects on organisms needs a multidisciplinary approach. With this in mind, and as an outgrowth of the EC MAST course *Ocean turbulence: a basic environmental property for plankton*, we review methods to generate turbulence in the laboratory and techniques to measure such turbulence in relation to their applicability to experiments with aquatic organisms. First we introduce several basic concepts to build a common ground for readers with a variety of backgrounds and interests. Then we discuss several methods to generate turbulence in the laboratory and mention the characteristics of the generated flows. We follow by describing different ways to estimate turbulence and we finish the chapter discussing a few topics that should be of interest to readers planning on doing experiments with organisms under turbulence. We will have fulfilled our objectives if this chapter is read by physicists and biologists alike and its reading develops into highly needed multidisciplinary research.

Key words: Small-scale turbulence, plankton, laboratory generated vs. oceanic turbulence, Kolmogorov microscales, laboratory experiments, grid-generated turbulence, Couette cylinders, energy dissipation rate, spectral density, integral length, hot-wire anemometry, Doppler anemometry, imaging methods.

INTRODUCTION

This chapter intends to give a glimpse of the methods used to generate and measure turbulence in the laboratory, in relation to biological experiments with small free-living organisms in the water. Its aim is to be a useful introduction to biologists on the treatment of turbulence as an environmental variable, and to serve as a starting point to design experimental setups to the newcomers in the field. It should also help physicists interested in biological problems to become familiarized with plankton and to start realizing the kinds of complexities biologists have to deal with when trying to answer relevant questions.

We realize that we are not going to be comprehensive in our treatment. This would require a whole book instead of a short chapter. For instance, there is a vast amount of literature on the distribution of plankton as affected by the combination of light, temperature and hydrodynamic regimes. Turbulence and mixing can be especially important in generating, maintaining and disrupting uneven dis-

*Received September 24, 1995. Accepted November 20, 1996.

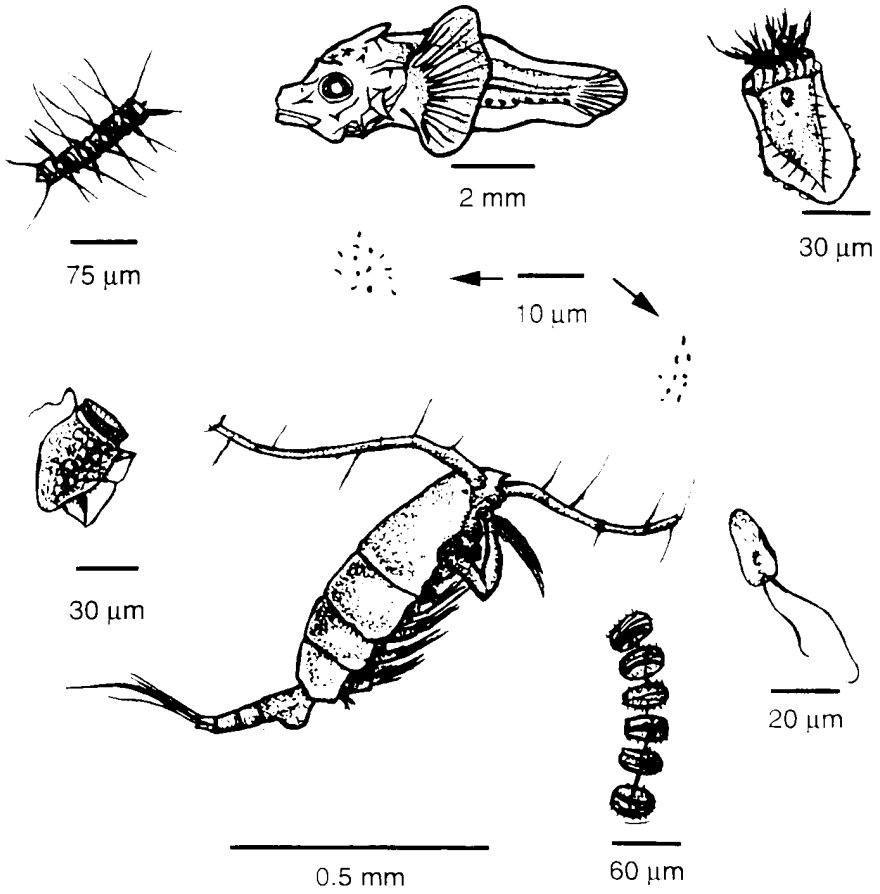

FIG. 1. Diversity of planktonic forms. Original drawings by Dr. Miquel Alcaraz.

tributions (patches) of planktonic populations (for a general reference see Rothschild (1988)). This is beyond the scope of the present review, which focuses more on the scales of motion that can be reproduced in the laboratory and that presumably can give more mechanistic answers to the processes observed in the sea.

We hope to spark more interdisciplinary science, which is greatly needed, especially from the biological point of view since so many biological phenomena are based on physical processes. From the physical point of view this interdisciplinary approach opens new venues for challenging research, where physical and engineering laws and principles need to be refined or modified to model a biological world of outstanding diversity and complexity. Organisms suspended in the water are for the most part still treated by modelers as uniform populations of spherical particles of equal size showing a uniform behavior, if any. This is far from realistic. Moreover, planktonic organisms can affect the physics from small and local scales such as by changing the viscosity of water (Jenkinson, 1993), to large or even planetary scales such as increasing the temperature of the ocean (Sathyendranath *et al.*, 1991) or modifying the Earth's albedo (Charlson *et al.*, 1987).

Plankton

Plankton is the community of organisms living in aquatic environments not in contact with limiting interfaces, and with a limited ability to overcome water movement at large scales. More powerful swimming organisms, generally larger, are referred to as nekton (Margalef, 1983). As one can readily see, the term *plankton* is not strictly defined. As confusing as it may seem, it is a term strongly rooted in aquatic biology, and is usually narrowed for specific groups of organisms based on taxonomy (e.g., zooplankton), size (e.g., microplankton), biochemistry or metabolism (e.g., phytoplankton) or other characteristics. The importance of studying plankton

and all the variables that affect the dynamics of its distribution becomes evident when one realizes that plankton dominates the biomass and the fluxes of material and energy in aquatic systems, having implications for such important issues as fisheries management and global warming, among others. Figure 1 shows some organisms representative of marine plankton.

Turbulence

Turbulence is a state of flow of a fluid characterized by stochastic movements in space and time. For instance, when measuring flow velocity (**u**) over time at a certain point in space, one can decompose **u** in a mean component (**U**) and a fluctuating term (**u**′), the latter giving the chaotic nature of the flow.

$$\mathbf{u} = \mathbf{U} + \mathbf{u}' \qquad (1)$$

This is called the Reynolds decomposition (bold face indicating that velocity is a vector). Turbulent flow is distinct from laminar flow for which average values of movement also determine the movement of each parcel of fluid. The kinematic viscosity (ν), an attribute of a fluid given by its molecular characteristics, opposes inertial motion and is very effective in damping out the smallest flow fluctuations. Hence, turbulent flow is dissipative, and it needs a constant energy source to maintain its random nature.

Turbulence can be considered homogeneous if the variance of the velocities does not change in space. Similarly, stationary turbulence is invariant in time and isotropic turbulence is invariant with respect to rotation (the variances of the velocities are equal for the different spatial directions).

Turbulence in the ocean

A variety of fluid motions, both organized and disorganized, occur in the ocean. There is a large variety of energetic inputs capable of causing these motions. The large scale currents in the sea, generated by the interaction between temperature and salinity differences and the Coriolis force are not turbulent in a strict sense as they are two dimensional (Tennekes and Lumley, 1972). Nevertheless, the term two-dimensional turbulence is used for these motions. In what follows we will not distinguish between two-dimensional pseudo-turbulence and fully developed three-dimensional turbulence.

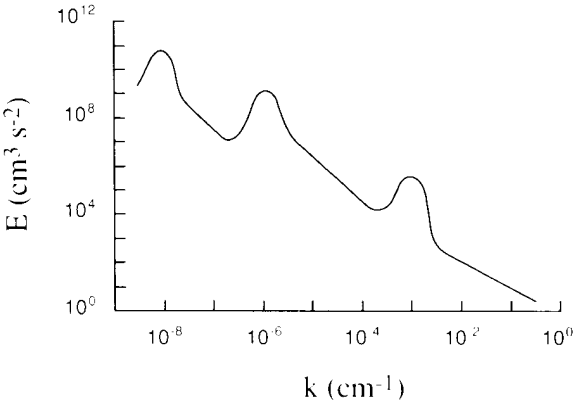

FIG. 2. – Sketch of the distribution of energy over different scales (after Okubo and Ozmidov, 1970). Inertial subranges, characterized by constant turbulent dissipation depicted as power laws, may have different slopes.

Turbulence occurs at a vast range of scales and is fueled by energy influxes at more or less discrete wavelengths. An energy peak around 10^6 m corresponds to energy from quasi-stationary cyclones and anticyclones. Disturbances of the order of 10^4 m are created mainly by the Coriolis and tidal forces. In the open ocean, the smallest energy input corresponds mainly to wind-driven gravity waves, at approximately a 10 m scale (Figure 2). Two excellent monographs on the subject are the ones by Phillips (1977) and Monin and Ozmidov (1985).

The eddies formed from these energy inputs are anisotropic, that is, horizontal turbulent fluctuations are many times larger than vertical ones. The anisotropy occurs mostly due to body forces (i.e. gravity or rotation), at least at the largest and smallest energy inputs (Figure 2). For the very large scales, say 10^5 m, the ocean has a flat aspect ratio and the main circulation is two-dimensional, thus, vertical motions are negligible when compared to the horizontal currents in the ocean. For the intermediate scales, say between 10^3 and 10^2 m, the anisotropy is usually forced by the density stratification, and eddies of those sizes are normally trapped between the surface of the ocean and the thermocline. In the two previous ranges the turbulence is basically bidimensional, and has an inertial subrange (region where the energy input from the larger scales is locally balanced with the energy loss to smaller scales) of the type $E \propto k^{-3}$, where k is the wavenumber and E is the energy per wavenumber (see Powell and Okubo, 1994).

There are several instabilities that cause the mainly two-dimensional eddies to break into smaller

eddies. Eventually, because of the chaotic nature of the process, including primary and secondary instabilities such as Kelvin-Helmholtz, Rayleigh-Taylor, etc. (Redondo and Linden, 1993), smaller eddies will lose their orientation and become locally isotropic. In the interval of the spectrum governed by local isotropy, energy is not substantially lost to heat through the effect of viscosity during eddy fractionation, rather it is transferred to smaller scale eddies. The turbulent energy is balanced by energy transfer from larger eddies and energy transfer to smaller eddies. This is determined by the rate of kinetic energy dissipation (ε) (see the section *Methods to measure turbulence* for further details). Energy dissipation rate is the decay of turbulent kinetic energy over time. At small scales where molecular forces become important, viscosity (ν) cannot be disregarded any longer, and eddies start to lose energy to heat. The breakpoint is known as the Kolmogorov microscale of space (λ_K), time (τ_K) and velocity (υ_K) and is determined as:

$$\lambda_K = \left(\frac{\nu^3}{\varepsilon}\right)^{1/4} \quad (2)$$

$$\tau_K = \left(\frac{\nu}{\varepsilon}\right)^{1/2} \quad (3)$$

$$\upsilon_K = (\nu\varepsilon)^{1/4} \quad (4)$$

The cascading process inherent to 3-D turbulence by which energy is transferred from the large (slow) to the small (fast) scales is quick. In the time of a few eddy turnover times the spectrum is filled with eddies of all sizes down to the Kolmogorov scale.

An example of the relationship of the microscales to ε can be seen in Table 1. Below λ_K viscous forces dominate water motion, which is characterized by a laminar shear field (Lazier and Mann, 1989).

TABLE 1. - Kolmogorov microscales with respect to turbulent kinetic energy dissipation rate. Microscales are calculated with Eqs. 2, 3 and 4 using a kinematic viscosity of 0.01 $cm^2\ s^{-1}$.

Turbulence ($cm^2\ s^{-3}$)	λ_K (cm)	τ_K (s)	υ_K ($cm\ s^{-1}$)
10^{-2}	1.8	320	0.0056
10^{-1}	0.56	32	0.018
10^{0}	0.18	3.2	0.056
10^{1}	0.056	0.32	0.18
10^{2}	0.018	0.032	0.56
10^{3}	0.0056	0.0032	1.8

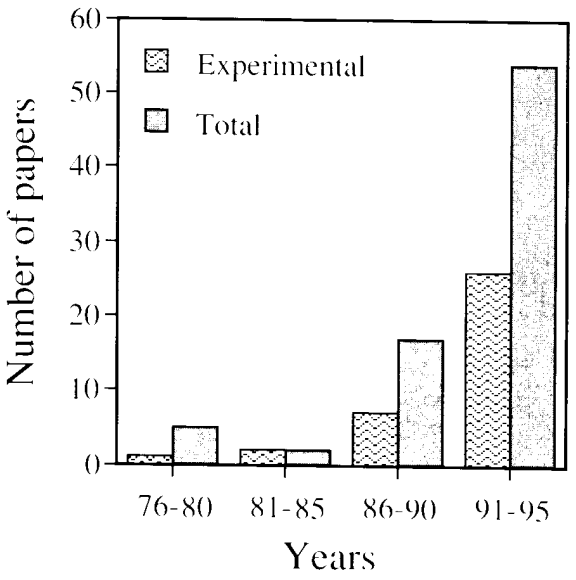

FIG. 3. - Evolution of the number of publications on the interaction of small-scale turbulence and plankton. Data collected from several bibliographic searches.

Relation of plankton to turbulence

The importance of turbulence as a source of auxiliary or external energy to pelagic environments has been hypothesized for some time (Margalef, 1978; Legendre *et al.*, 1986). Other than to keep recording physical and biological data and finding significant correlations among different variables, testing these ideas from a whole system approach is not viable, at least in the ocean. The effects observed at the aquatic ecosystem level have their origin in the interactions of the physical processes governing the movement of water and the transport of scalars with the different biological components (from individual organisms to populations and communities). Planktonic organisms move by swimming or other means, feed by taking up nutrients and/or eating particles, grow, reproduce, and in a word, live in an environment in turbulent motion, at least for part of the time. From an evolutionary point of view, it is expected that organisms have adapted to sense, and take advantage of and/or avoid the different hydrodynamic regimes they encounter. Lately, an increasing number of studies (Figure 3) are taking a bottom-up approach to test the interactions of turbulence and plankton, focusing mostly on experiments in microcosms in which a certain hydrodynamic regime is created and its effects on some biological component or process is determined.

APPROACHES TO STUDY TURBULENCE AS AN ENVIRONMENTAL FACTOR FOR PLANKTON

In order to experimentally study the effects of turbulence on planktonic organisms we can follow one of two approaches, as already hinted in the previous section. One is to sample nature assuming it is doing an experiment for us, and the other is to do the experiment ourselves. We will shortly discuss both approaches, and then focus on ways to measure and to reproduce turbulence in the laboratory for experiments with plankton.

Sampling nature

We can measure turbulence as well as biological variables or processes in aquatic systems to obtain a large body of data for a range of turbulent conditions. Empirical relationships are then found between physical and biological variables using statistical methods of analysis. These models can then be used for predictive purposes provided the data set is quantitatively as well as qualitatively extensive enough. In our view, the power of this approach lies in two aspects. First, the observed biological responses are integrated results of the effects of turbulence at the system level, giving a 'big picture' scope of the problem. However, since one cannot control variables that are extraneous to the study, results may be masked so much as to obscure the relationship between turbulence and the biological variables of interest. Second, the results of these models should be most useful as good grounds to build testable hypothesis.

In the ocean and other large water bodies one is at the whim of gathering data whenever the weather permits, obtaining a truncated range for both the experimental variable and the response variables. It is also difficult to see and study any time lags in the biological responses unless one tracks the water masses. Additionally, research cruises are rarely multidisciplinary, and when they are, it is difficult to match appropriate sampling schedules for physicists and biologists. Still, we should be able to find solutions to sampling differences under some compromise.

As examples of such an approach, Sundby and Fossum (1990) and Ottersen and Sundby (1995) related the number of prey in cod larval guts (a measure of feeding) to the concentration of free swimming prey and to wind speed, for data gathered over a 8-year period in the Norwegian Arctic. They found that turbulence above a certain level probably increased the contact rate between cod larvae and their prey, which in turn enhanced feeding. Turbulent energy dissipation rates were not measured directly in these studies but calculated from wind speeds. Other studies include those of Maillet and Checkley (1991) and Gallego *et al.* (1996).

Setting up experiments

The second approach is to do experiments in microcosms. Microcosms, as we understand it, are bio/ecological systems or parts of systems enclosed in a relatively small container or boundary. Larger containers may qualify as mesocosms. The macrocosm or simply, cosmos, would refer to the natural system with whatever boundaries it had or did not have. The distinction is generally based on the relative size and time scales of the organisms/systems of interest enclosed in the container with respect to the scales of the container itself. A 5000 m^3 container may qualify as a microcosm if the organisms studied are sharks. For a further discussion on the use of microcosms see Giesy (1980).

In microcosms, we can control the turbulence levels and measure the effects on any biological variable of interest. However, one has to keep in mind that the physiology and behavior of the simplest organism is the result of a myriad interactions. Controlling any additional factors (e.g. temperature, light, nutrient and/or food supply, etc.) will be of greatest importance to discern the effects of turbulence levels in laboratory experiments. Think for a moment about temperature, which besides affecting any metabolically related process, affects the viscosity of the fluid and thus the Kolmogorov microscales. We will not discuss the biggest drawback of this approach, namely the difficulty of extrapolating results to natural conditions when using the microcosm as a model of a whole ecosystem (see Giesy, 1980). What we can do with accurate laboratory experiments is to understand the mechanisms of interaction between turbulence and some component of plankton.

On the methodological side, the main problem is to generate turbulence in a way that is comparable both in intensity and in quality to that observed in natural systems. As far as intensity is concerned, turbulence levels that have been used in the laboratory are skewed to high levels as compared to naturally occurring turbulence (Figure 4). When the charac-

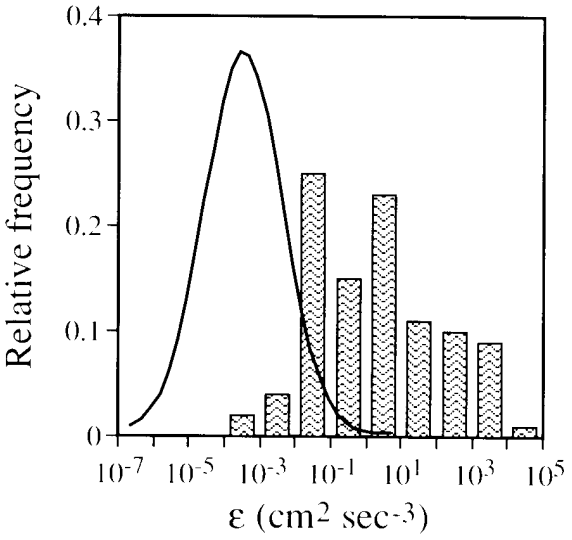

FIG. 4. Comparison of turbulence levels in the surface mixing layer of the ocean (line, after MacKenzie and Leggett, 1993) to turbulence levels used in experiments with planktonic organisms.

teristics of turbulence are considered, plankton in nature usually live in a homogeneous and isotropic environment, unless the organisms are close to an interface. This is also hard to completely achieve in microcosms where the ratio boundary/volume is much higher. See the discussion section for further treatment of this topic.

METHODS TO GENERATE TURBULENCE

Grids

Laboratory experiments using grids to generate turbulence are of two types. First, those where the turbulence is generated by an oscillating grid and the mean flow in the experimental container is zero, and second, those produced by a one-off energy release, as in the dropping of a grid, where the turbulence decays in time and goes through a continuous change of scales. Extensive discussion of these experimental techniques is given in the book by Turner (1973) and more recently in reviews by Hopfinger (1987) and Fernando (1991), mostly with application to density stratified flows.

Oscillating grid turbulence

For physical oscillating grid experiments, which were initially done by Rouse and Dodu (1955) and Turner (1968, 1973) in the context of entrainment measurements in stratified flows, the characteristics of the turbulence have been very well studied. In these experiments, the entrainment velocity (V_e) of the turbulent front that propagates outwards from the grid as it begins to oscillate is defined as:

$$V_e = \mathrm{d}D/\mathrm{d}t \ , \qquad (5)$$

where D is the extension of the turbulent layer, depending on the initial stratification of the tank, if any, and is given by a simple law of the type

$$E = c\,\mathrm{Ri}^{\,n} \qquad (6)$$

where E, is the entrainment rate defined as $E=V_e/V$ (V being some global or local reference velocity) and c and n are experimental constants. The Richardson number, Ri, measures the relative importance of buoyancy forces which usually act to stabilize the flow, and velocity fluctuations which tend to destabilize it. The Richardson number can be defined in various ways, the most relevant one based on local parameters, such as, u' (the root mean square, r.m.s., turbulent velocity) and l (the integral length scale of the turbulence)

$$\mathrm{Ri} = \frac{g\,\Delta\rho\,l}{u'^2} \qquad (7)$$

where $\Delta\rho$ is the buoyancy jump across a density interface. The limiting entrainment for a non stratified flow (Ri = 0) is E = 0.5, where Eq. 6 is no longer valid.

The detailed turbulence produced by a type of oscillating grid, used by Turner with mesh M = 5 cm formed out of square bars 1 cm thick has been studied by Thomson (1969), McDougall (1979), Hopfinger and Toly (1976) and Redondo (1988).

To evaluate the effect of the grid on flow it is necessary to know the velocity and length scales characteristic of the generated turbulence. Thomson (1969) was the first one to obtain detailed measurements of turbulence generated by an oscillating grid. He used a hot wire anemometer. To overcome the lack of a mean velocity of the flow (see the section *Measuring flow velocity time series*) he moved his anemometer in a circular motion at different distances from the oscillating grid.

Thomson (1969) used grids with a 5 cm mesh (M) and 1 cm wide bars. McDougall (1979) repeated Thomson's experiments with a laser velocimeter and found some lateral inhomogeneities. Thomson and Turner (1975) show the empirical relationships:

$$l = \beta z \tag{8}$$

for the integral scale of turbulence, and

$$u' = 1.4\,\omega s^{5/2} z^{-3/2} \tag{9}$$

for the r.m.s. velocity, where Z is the distance from the grid, S is the amplitude of oscillation, ω the frequency of oscillation, and β is a proportionality constant that weakly depends on S; for $S = 1$, $\beta = 0.10$.

Later Hopfinger and Toly (1976) considered the following expression to be more appropriate:

$$\frac{u'}{\omega s} = c\, s^{1/2} M^{1/2} z^{-1} \tag{10}$$

This last expression, which needs to be calibrated for each grid type to estimate c, has been verified by several authors (Hannoun and List, 1988; Redondo, 1988; Fernando, 1991).

Dropping grid turbulence

Most of the turbulence in the real world is non-stationary, as one rarely observes a continuous supply of mechanically generated turbulence. Grid generated turbulence has long been used because of the simplicity of the turbulence that is produced. Two experimental approaches have been taken in order to study the decay of the turbulence behind a grid: 1) moving the fluid with respect to the grid, as in a wind tunnel or water channel, and 2) moving the grid in the fluid.

The advantage of the first approach is the possibility of using hot wire or hot film velocity probes in order to measure buoyancy fluxes in a stratified fluid. With the second approach it is easier to maintain a closed environment inside a container with fixed mass. This last type of experiment has been performed in stratified flows with the grid falling perpendicular to the interface in Linden (1979), Dickey and Mellor (1980) and Linden (1980), or towing a grid parallel to the interface as in the experiments by Lin and Pao (1979), Britter *et al.* (1983) and Britter (1984) among others.

As the grid passes, the turbulence decays in time. As we look further downstream, the turbulent length scale increases and the velocity decreases, and we are left with a non-stationary system. Batchelor and Townsend (1948 a, b) obtained the following relationships, both theoretically and experimentally. For the initial period of turbulence decay:

$$u' \propto t^{-1/2} \tag{11}$$

$$l = (10\,\nu)^{1/2} t^{1/2} \tag{12}$$

and for the final period of decay

$$u' \propto t^{-5/4} \tag{13}$$

$$l = (4\,\nu)^{1/2} t^{1/2} \tag{14}$$

Tan and Ling (1963) expressed doubts about the change in velocity for the final period and suggested that $u' \propto t^{-1/2}$ throughout. Batchelor and Stewart (1950) showed that the large scales behind the grid in a uniform flow are anisotropic so that u'^2/w'^2 tends to 1.5 at a sufficiently large distance from the grid.

The effects of stratification on turbulence has been studied by Dickey and Mellor (1980), Lin and Pao (1979) and Britter *et al.* (1983). In their experiment Dickey and Mellor used a unidimensional grid moved vertically upwards, and perpendicularly to the interface. They clearly observed internal waves ($Ri > 12$), and an increase in the vertical r.m.s.

Lin and Pao (1979) and Britter *et al.* (1983) towed a vertical grid parallel to the interface. They did not observe internal waves up to much higher Richardson numbers. Lin and Pao observed that the anisotropy increased with time, from $u'^2/w'^2 = 1.8$ to 11. Stillinger *et al.* (1983) however, observed that $u'^2/w'^2 \leq 1.15$ suggesting anisotropy at large scales.

It is common in experiments to consider the mesh of the grid as the initial characteristic scale of turbulence ($l = M$), and the turbulent velocity initially generated to be proportional to the falling velocity of the grid ($u' \propto U$). However, one should be aware of some anisotropy in the turbulence at the wake of the grid.

Biological experimental uses

The oscillating grid approach (Figure 5) has been reported extensively in the biological literature, not only as a means to generate turbulence as an experimental variable but also to keep organisms in suspension and simulate upper ocean mixing layers in microcosms (Nixon *et al.*, 1980).

Howarth *et al.* (1993) used cylindrical tanks (3 m^3, 1.83 m in Ø) with an oscillating grid (Figure 5a) to assess the effect of turbulence on the rate of nitrogen fixation by cyanobacteria. Landry *et al.* (1995) had a horizontally moving grid system to study the effect of small-scale turbulence on the ingestion rate

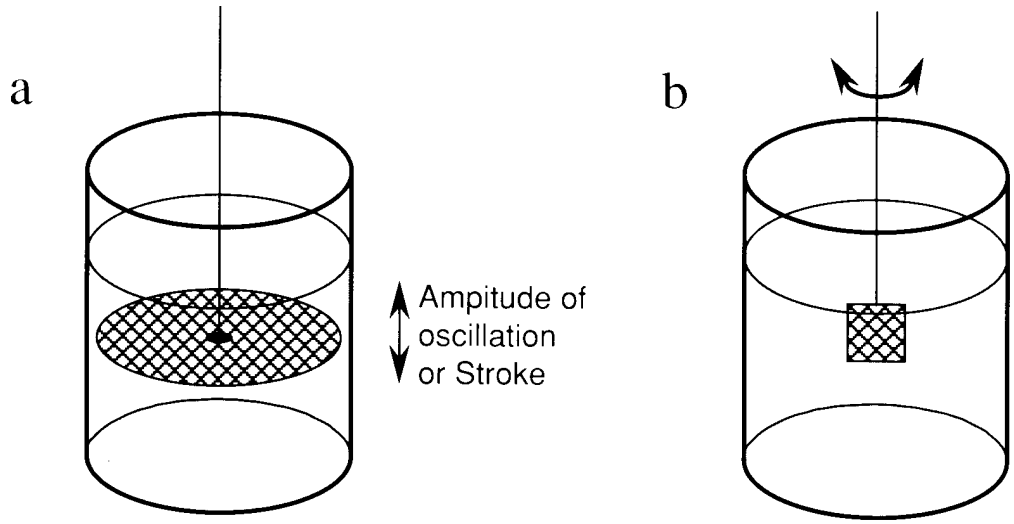

FIG. 5. Drawing of two different grid-generated turbulence set-ups. (**a**), vertically oscilating grid. (**b**), axis-symmetrically oscillating grid

of fish larvae, and applied Eq. 10 to obtain the turbulent velocity. MacKenzie and Kiørboe (1995) also used an oscillating grid but had a screen between the grid and the fish larvae, to avoid damaging the organisms. In this case, the equations of the section *Oscillating grid turbulence* are not valid, and turbulence was estimated by other methods. Estrada *et al.* (1987) and Alcaraz *et al.* (1988) used oscillating grids in the upper portion of their 30 dm^3 microcosms to simulate an upper mixed layer. Saiz and Alcaraz (1991) used a similar approach in 10 dm^3 microcosms but instead of one they had two oscillating grids in series. Savidge (1981) used a reciprocating grid with a constant travel velocity to assess the growth of some phytoplankton species under turbulence. Berdalet (1992), Saiz *et al.* (1992), Peters and Gross (1994), Saiz and Kiørboe (1995), Peters *et al.* (1996) have used grids at various oscillating rates and generally large strokes (close to the container height) to study the effects of turbulence on a variety of organisms and biological processes (from cell division in dinoflagellates to feeding in protozoa and in copepods). Oscillating grid equations cannot be used in this case to predict the level of turbulence at a distance z away from the grid, since z is continuously changing.

Biologists prefer cylindrical tanks for their experiments and grids with dimensions adapted to their needs, while most physical experimentation is done with square-based tanks, and standard size grids. Cylindrical tanks tend to ensure more homogeneous spatial conditions for the organisms (for instance, light conditions could be different in corners). Physicists use square tanks because the corners break possible secondary mean flows and visualization is straightforward. Hence when applying the equations from the literature to setups for biology, the calculated values have to be used with caution.

Vibration

The principle of this method consists of introducing kinetic energy into the experimental recipient by means of a vibrating object submerged in the water. The first system developed consisted of the motor of an electric toothbrush for which the brush had been replaced by three metal pins (Costello *et al.*, 1990; Marrasé *et al.*, 1990). Alcaraz *et al.* (1994) and Saiz and Alcaraz (1992 b) used a similar system but attached a small piece of netlon grid vertically, that oscillated in the x-y plane at high frequency. A range of frequencies of oscillation can easily be achieved with a thyristor. The highest energy dissipation rates are measured close to the source of vibration and they decay away from it in all directions, giving a non-uniform spatial distribution of energy dissipation rates in the container. There are also some very clear secondary flows generated within the container (Enric Saiz, pers. comm.). The decay of fluctuating velocities for point vibrators is similar to that for grids. The *action of the grid or vibrator*, $A=\mathbf{u}'d$, with dimensions of diffusivity, is constant with distance d from the source; hence an inverse relationship of $\mathbf{u}'$ and d is shown.

Shakers and stirrers

Stirrers have not been used to assess turbulence effects on planktonic organisms, even though coated magnetic rods gyrated in a container by an outside magnetic stirrer motor are widely used to culture phytoplankton, especially diatoms. However, stirrers and propellers of different kinds are used extensively to study the coagulation, mechanical damage, and other parameters of turbulence on suspensions of cells (non-planktonic). This is done mainly to optimize the growth and/or excretion of some substance of interest of mammalian and other cells in bioreactors (Toma *et al.*, 1991; Thomas *et al.*, 1994; Moreira *et al.*, 1995).

Shakers were preferred devices to generate turbulence treatments in early biological experiments, mainly because they could be bought off the shelf and were already used in culturing laboratories. The shaking motion can be orbital or reciprocal (back and forth) and shakers can be obtained with fixed or variable speeds. They have been used to create turbulent motion in experiments with dinoflagellates (White, 1976; Pollingher and Zemel, 1981; Berdalet, 1992), but also for other organisms such as copepods (Saiz and Alcaraz, 1992a), protozoa (Hellung-Larsen and Lyhne, 1992) and bacteria (Moeseneder and Herndl, 1995).

Turbulence in a shaker is produced by wall effects in the flask and the relevant viscous length scale can be written as:

$$l = \left(\frac{\nu}{\omega} \right)^{1/2} \qquad (15)$$

where l is the depth of the viscous layer to the container wall, ν is the kinematic viscosity, and ω is the angular velocity. One has to ensure that l is sufficiently small in order to have a sizable turbulent field.

The types of vortices shed by an oscillating boundary layer (such as a flask with water inside) are symmetrical, advancing into the body of the fluid from the boundaries. Thus one also has to make sure that the turbulence generated at the oscillating boundaries penetrates into the bulk of the fluid. This will be fulfilled if the maximum distance to any boundary is less than l_t, defined also by Eq. 15 but substituting the molecular viscosity by a, hopefully measured, turbulent viscosity (ν_t) as defined by Boussinesq (Launder and Landry, 1972). In the case of an orbital shaker, the type of instabilities shed from the walls are of Tollmien-Schlichting type, which appear in shear flows but obey a circular pattern. In both of these cases the level of turbulence is stronger near the walls of the container.

Couette cylinders

A Couette cylinder consists of two coaxial cylinders which leave a small gap that is filled with a fluid. The two cylinders are rotated at different angular speeds, giving shear rates which increase with the difference in angular speeds. Under appropriate dimensions and speeds, this creates a laminar shear field between the two sheets. The use of Couette cylinders in experiments with plankton has been popularized by the uniformity of its flow conditions and by the ready calculation of shear parameters for different settings without the need to do any physical measurements. It has been supported by the theoretical reasoning that organisms that are smaller than λ_K (most planktonic organisms under non-stormy conditions) are not affected by the random fluctuations in the velocity field but only by the remaining laminar shear field (Lazier and Mann, 1989; Thomas and Gibson, 1990 b; Shimeta *et al.*, 1995).

The movement of a viscous fluid between two cylinders with independent rotation has been a classical problem of fluid mechanics. Based on the drawing of Figure 6 the parameters and variables of interest of the system are as follows. Geometric

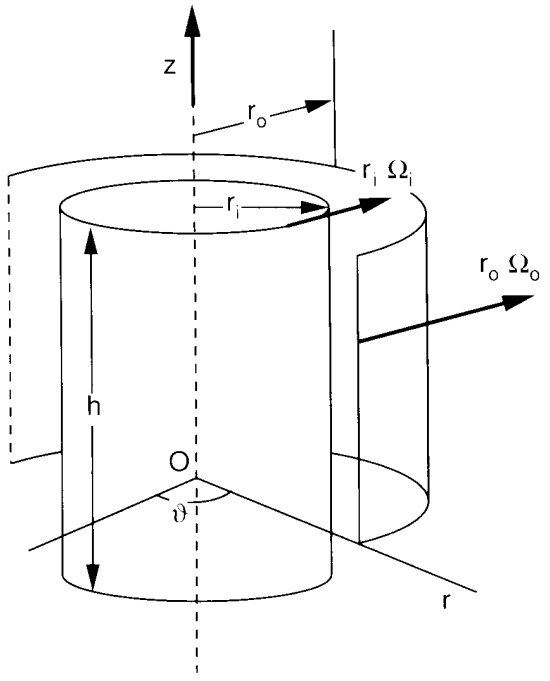

FIG. 6. – Sketch of a Couette cylinder showing the relevant parameters and variables.

parameters are the internal radius (r_i) the external radius (r_o), the difference between those two radii ($d=r_o-r_i$) and the height of the cylinder (h). Physical variables include the kinematic viscosity of the fluid (ν), the velocity ($\mathbf{u}$) and the pressure (p) of the fluid at a point and the angular velocities of the inner (Ω_i) and outer (Ω_o) cylinders.

The independent non-dimensional numbers that can be calculated are the ratio of radii (η), the aspect ratio (Γ), and the inner (Re_i) and outer (Re_o) Reynolds numbers:

$$\eta = \frac{r_i}{r_o} \tag{16}$$

$$\Gamma = \frac{h}{d} \tag{17}$$

$$\mathrm{Re}_i = \frac{\Omega_i r_i d}{\nu} \tag{18}$$

$$\mathrm{Re}_o = \frac{\Omega_o r_o d}{\nu} \tag{19}$$

where η and Γ are useful to characterize the type of dominant instability that takes place at different ratios of angular velocities, ζ

$$\zeta = \frac{\Omega_o}{\Omega_i} \tag{20}$$

and at different Taylor numbers, T

$$T = \frac{4\Omega_i^2 d^4}{\nu^2}\left(\frac{\eta^2-\zeta}{1-\eta^2}\right) = $$

$$= 4\,\mathrm{Re}_i^2\left(\frac{d}{r_i}\right)\frac{\eta}{1-\eta}\left(1-\frac{\zeta}{\eta^2}\right) \tag{21}$$

We show in Figure 7 the diversity of flow patterns appearing in a Couette cylinder. In the parameter space given by the Re_i and Re_o there is a very wide variety of different dominant instabilities that characterize the flow. Thus, the turbulent characteristics can not vary continuously by just increasing the angular velocity as there are sharp transitions dominated by instabilities such as (say for $\mathrm{Re}_o \approx 500$) Taylor vortices, wavy outflow and wavy inflow, wavy vortices, and corkscrew vortices. It is important to know exactly in which parameter range is the Couette flow operating and which are the dominant instabilities that generate the small-scale motion.

When Couette devices have been used in biological experiments (Thomas and Gibson, 1990 a, b; Thomas and Gibson, 1992; Gibson and Thomas, 1995; Mead and Denny, 1995; Shimeta *et al.*, 1995; Thomas *et al.*, 1995), Couette flow seems to have been ensured. The inner cylinder is always kept stationary so that $\mathrm{Re}_i = 0$ and we are in the

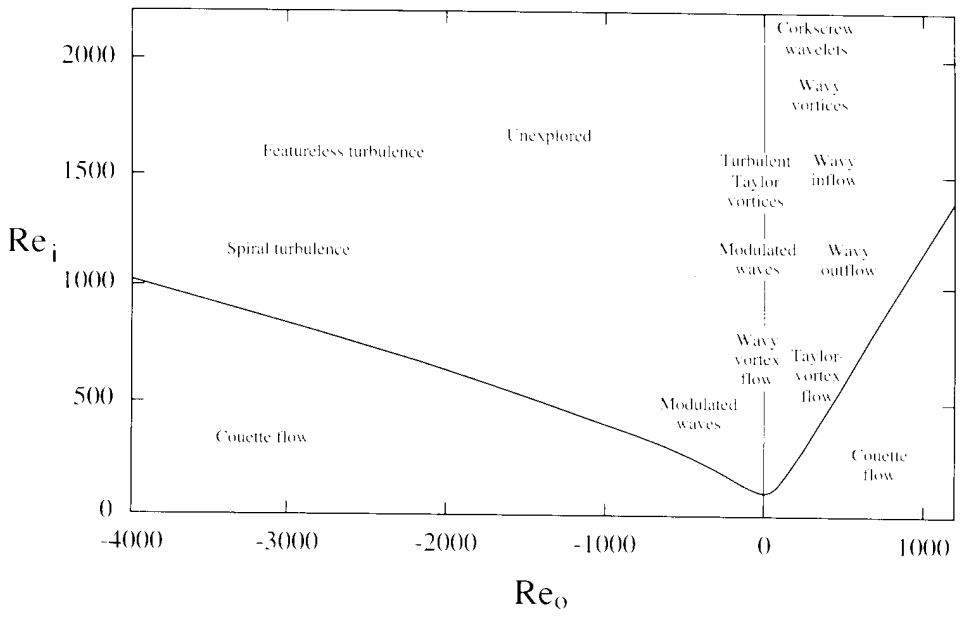

FIG. 7. Diagram of flow types in a Couette device depending on the Reynolds numbers of the outer and inner cylinders. Negative Re used by convention to denote opposite rotation directions of the two cylinders. $\eta = 0.88$. After Tritton (1988).

region of pure Couette flow (Figure 7), although we have to be cautious in extrapolating the results shown in this diagram since they were obtained for a specific dimensional setting and Γ between 20 and 48, and a specific range of Re_a. The shear stress, τ, between the two cylinders for such a setup is given by

$$\tau = \mu\left(\frac{\Omega_o r_o}{d}\right) \tag{22}$$

where μ is the dynamic viscosity of the fluid (M L^{-1} T^{-1}). The energy dissipation rate may be given as

$$\varepsilon \propto \left(\frac{\tau \nu^4}{\rho}\right)^{1/2} \tag{23}$$

Eqs. 22 and 23 apply both under laminar and turbulent conditions, if we substitute ν by ν_t flows inside the Couette cells (Schlichting, 1979).

Other methods

Shear-free methods

A standard method for generating turbulence is to use buoyancy. This is usually done by convective heating or cooling at a surface of the container. If the heat is applied at the bottom of the tank, Rayleigh-Benard cells appear at a critical Rayleigh number (Ra) (1780 for a completely full tank) defined in terms of the temperature difference (Δt) between the top and bottom of the tank as:

$$\mathrm{Ra} = \frac{g\alpha\Delta t L^3}{\nu\kappa} \tag{24}$$

where g is gravity, α is the volumetric heat expansion coefficient, L is the height of the tank and κ is the temperature diffusivity. As Ra increases the flow becomes more turbulent. Similar instabilities occur by heating or cooling the sidewalls (for further references see Tritton, 1988). The main inconvenience of this system in biological applications is the heat gradients which appear within the fluid.

Another method of generating turbulence by means of buoyancy differences may be to use a single plume in the experimental tank. The buoyancy flux of the plume is defined as

$$B = g\frac{\Delta t}{t}Q \tag{25}$$

where Q is the volume flux which enters the tank at a temperature difference Δt from the ambient temperature. As described in Turner (1973), the vertical velocity (w) at the center of the plume at height z is given by:

$$w = B^{1/3}z^{-1/3}, \tag{26}$$

an upper limit for ε can be estimated as

$$\varepsilon \propto \frac{w^3}{z}.$$

Injection of air bubbles is sometimes used to generate turbulence (Durst *et al.*, 1986). The relevant scale is that of the spatial separation between the bubbles, as half of that distance shows the maximum turbulent shear in the flow

$$\frac{\partial u'}{\partial x} \propto \frac{2v_r}{d} \tag{27}$$

where v_r is the rise velocity of the bubbles and d the average distance between them. The turbulent energy input may be controlled by changing the air flow as well as the rise of the bubbles. An estimate of the rate of energy dissipation may be made by taking into account the work done on the fluid by the drag of all bubbles.

Shear generated turbulence

A well known method of generating turbulence is from the shear of the mean velocity in the fluid. In the previous subsections we have reviewed some of the work done on the effect of mechanically generated turbulence, where turbulence is generated by grids in a shear free environment. In a similar way turbulence can be generated by resonant waves as in McEwan (1983) or some form of external input of energy in the system. When there is a mean shear in the flow, turbulence can be generated by extraction of energy from the mean flow by means of the Kelvin-Helmholtz instability and associated instabilities. When there is a density interface, and a mean velocity shear across it produces mixing, the process is normally referred to as internal mixing, Turner (1973).

The direct contribution to turbulent energy from the shear of the mean flow may be calculated as, say for a vertical shear

$$P = \overline{u'w'}\frac{\partial \bar{u}}{\partial z} \tag{28}$$

None of these methods have been used in biological experiments, mainly because of the inhomogeneity inherent in their setups.

METHODS TO MEASURE TURBULENCE

When trying to assess the importance of any physical variable on organisms one has to be able to measure this physical variable, as a reference both to other studies and to the range of values the variable has in the natural environment. But how does one measure turbulence?

In order to characterize the turbulence the probability distribution functions of the velocity $P(u)$ are used to calculate the moments (M_i, i meaning the moment number) of the velocity

$$M_i = \int u^i P(u)\,\mathrm{d}u \tag{29}$$

noting that the second moment is the variance, the third order is the skewness and the fourth order, the flatness.

From the spatial and temporal autocorrelations, and their FFT's (Fast Fourier Transform), the spectra are calculated. The dissipation ε defined above, appears in the turbulent energy equation, which may be written in a simplified form as

$$\mathrm{d}q/\mathrm{d}t = T + P + B - \varepsilon \tag{30}$$

where q is the turbulent kinetic energy, T is the turbulent kinetic energy transport, P is the production, often due to shear, and B the buoyancy, source or sink if the fluid is stratified (see Gargett, 1997, for more details).

Both in the production and buoyancy terms, turbulent fluxes appear as correlations $\overline{u_i'u_j'}$, which indicate the flux of i directed momentum in the j direction or vice versa due to the symmetry of the Reynolds stresses (Redondo, 1987). The same happens with density $\overline{u_i'\rho}$. The turbulent diffusivities or viscosities, ν_t, are defined as

$$\overline{u_i'u_j'} = \nu_t \left(\frac{\mathrm{d}u_i}{\mathrm{d}x_j} + \frac{\mathrm{d}u_j}{\mathrm{d}x_i} \right) \tag{31}$$

and are also used to characterize the mixing ability of turbulence (see the discussion).

The dimensions of turbulent kinetic energy dissipation rate (ε) are L^2T^{-3}. Where do these dimensions mathematically come from? A rate of change of energy will have the dimensions of energy/time. So: $ML^2T^{-2}/T = ML^2T^{-3}$. The mass term is dropped, a common practice in fluid dynamics. Generally used units in oceanography are: W Kg^{-1}, mW Kg^{-1}, and $cm^2\ s^{-3}$. A widely used variation is to consider the rate per unit volume instead of per unit mass (Table 2). The transformation is achieved multiplying by the density of the fluid considered.

TABLE 2. Correspondence of units that measure turbulent kinetic energy dissipation rate with W Kg^{-1} as reference.

Unit	W Kg^{-1}	mW Kg^{-1}	cm^2s^{-3}	W m^{-3}
Correspondence	1	1000	10000	1025*

*Approx. for seawater of 35 psu and 20 °C.

How can one measure ε? It is usually done from measurements of flow velocity fluctuations. So the first problem is to measure flow velocity. Data has to be gathered at a spatial and temporal resolution according to our needs and in relation to the scales of the organisms we are dealing with. The spatial resolution will depend basically on the physical dimensions/characteristics of our probe or measurement device. The temporal resolution will depend on a number of things but basically on the time response of our probe and associated electronic circuitry, and our data sampling frequency. Suffice it to say that in order to resolve fluctuations of a certain frequency we need a sampling frequency of at least twice our frequency of interest (Nyquist sampling theorem). Below we are going to focus on the methods to measure turbulence in the laboratory. Clifford and French (1993) reviewed the instruments normally employed to acquire geophysical turbulence data in the field and the methods to analyze the data, and is an excellent source for additional information.

Measuring flow velocity time series

In general, one uses a sensor at a fixed point in space to measure time series of flow velocity. The Reynolds decomposition (Eq. 1) can then be applied to obtain the average velocity and the time series of the fluctuating component of velocity. For calculation purposes that we will see below the fluctuating component of the velocity series should be small compared to the average velocity of the flow. When this is not possible, such as in an oscillating grid system with zero average velocity, one can move the sensor through the fluid at a constant high velocity. The fluctuations will then become small compared to the measured mean velocity. How do we obtain ε from these measurements?

Basic estimates of ε.

From the definition of dissipation

$$\varepsilon = \nu \overline{\nabla \mathbf{u}' \nabla \mathbf{u}'} \tag{32}$$

(Tennekes and Lumley 1972) it is necessary to calculate the velocity gradients, but most times a dimensional analysis approximation is used

$$\varepsilon = c \frac{u'^3}{l} \tag{33}$$

where c is a constant and l is the integral length scale, a measure of the size of the most energetic eddies in the flow. This length scale can be obtained from the spatial velocity correlation, when we have simultaneous measurements at two points separated a distance r, as

$$l = \int \overline{u'(x)u'(x+r)}\,dr \tag{34}$$

or from even coarser estimates. For example, when having a grid generating turbulence in a container, l could be chosen as the mesh size of the grid. In any case, l cannot be larger than the largest dimension of the container, thus obtaining a minimum estimate for ε.

It is important to know when the viscosity drain of energy stops the turbulent cascade, both for the velocity (λ_k) and for the scalars like temperature or salinity. The Prandtl-Schmidt number, PrSc=ν/D, where D is the diffusivity of the scalar, defines the presence of the Batchelor scale, $\lambda_B=\lambda_k \mathrm{PrSc}^{-1/2}$ (if PrSc>1) or the Corrsin scale, $\lambda_c=\lambda_k \mathrm{PrSc}^{-3/2}$ (if PrSc<1). In Figure 8 we see how the different scales modify the scalar inertial subrange to a diffusion subrange.

Spectral analysis

With the velocity time series one finds the energy spectrum, which gives a plot of energy as distributed in the different frequencies or in the different wavenumbers ($k=2\pi/\lambda$). To obtain a spectrum (E, units of L^3T^{-2}) such as the ones in Figure 8 one has to apply a Fourier transform to the autocorrelation function of the velocity time series. To transform the frequency axis into a wavenumber axis the former has to be divided by the mean velocity ($\mathbf{U}$). For this transformation to hold, $\mathbf{U}$ has to be constant and $\mathbf{U}>>\mathbf{u}'$. One obtains a relationship of $E(k)$ versus k. It turns out that in the regions of local isotropy $E(k)$ is proportional to $k^{-5/3}$, and the relationship is

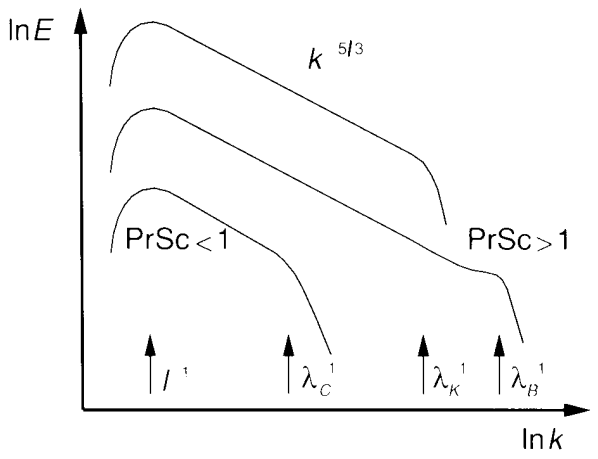

FIG. 8. Description of the inertial subrange and the diffusive subranges near the Kolmogorov lengthscale. The three spectra have been offset in the ordinate axis for display purposes. Note that for salt and heat (with diffusivities of 1.5×10^{-9} and 1.5×10^{-7} m^2 s^{-1} respectively) in the ocean, PrSc>1.

$$E(k) = c\,\varepsilon^{2/3} k^{-5/3} \tag{35}$$

where c is an empirical constant of ca. 1.4. The energy dissipation rate can then be readily calculated. Howarth *et al.* (1993) calculated ε applying a formula in Tennekes and Lumley (1972), derived by Fourier transforming Eq. 30.

$$\varepsilon = 2\,\nu \int k^2 E(k)\,\mathrm{d}k \tag{36}$$

This method was used by Howarth *et al.* (1993) to calculate the dissipation in their experimental tanks. They were limited to obtain velocity time series data in the upper centimeters of their tank where the oscillating grid that was generating the turbulence was not physically interfering with the moving probe, thus, most likely, underestimating the average energy dissipation in the tank.

Hot wires, hot films, and thermistors

These devices have been used for a long time to measure flow. They are elements that are heated. Their operating principle is based on a strong dependence of their cooling on the speed of flow past them. Hot wires and films are made of a metal (e.g. platinum) while thermistors are semiconductors. In both cases the resistance of these elements is a function of temperature. When appropriately connected to electric/electronic circuitry the change in resistance owing to the cooling in the flow can be transformed into a signal which can be recorded.

Calibration of these devices is a major issue since it is highly dependent on each probe and the response of temperature to flow speed is not always linear. In general, hot wires and films are highly sensitive to rapid flow fluctuations, but are also very fragile. More rugged probes can be built with thermistors (LaBarbera and Vogel, 1976; Vogel, 1989). Thermistor based systems can measure fluctuations at very low flow speeds but their time response is not as good as that of hot wires and films. However, semiconductor technology keeps improving and we can expect very fast response times from thermistors in the future. Perhaps one of the major problems of all these devices is their rapid fouling. Substances (particulate and dissolved) stick to them very easily, the sensitivity rapidly decreasing, and they have to be cleaned and recalibrated.

These devices give a response dependent on the flow past them but they cannot sense the direction of this flow (Bradshaw, 1979). Furthermore, the probes tend to be very sensitive to flow direction, that is, they will measure very differently if positioned parallel to the flow or perpendicularly to it. To separate the different spatial components of velocity one needs more than one sensor, strategically positioned to measure preferentially different velocity components. One can readily see that, there will be physical positioning constraints if the need is to measure simultaneously the different velocity components of the same small parcel of water. The so called omnidirectional probes are somewhat less sensitive to flow direction.

Laser Doppler Velocimetry

Time series data can also be obtained using a LDV or LDA (Laser Doppler Velocimeter or Anemometer). The LDV measures the interference pattern, produced by suspended particles in the fluid, between the incoming and outgoing beams. The velocities of a large number of particles can be measured in a few minutes almost effortlessly. The sampling volume is very small (0.1 to 1 mm^3), and one has to play with the concentration of reflecting particles so as to have enough particles that cross the sampling volume for a particular sampling frequency, and not too many particles so that there would be more than one per sampling volume. Each spatial dimension requires its own laser beam, and they are all focused to a single spot to get simultaneous measurements for the different velocity components. Two dimensions are generally used to characterize the flow, assuming the velocities in the third dimension equal those in one of the other two dimensions. There is no impediment to using three lasers and truly obtain tridimensional data on velocities other than the price tag and a much greater difficulty in aligning the lasers to a single spot in space.

LDVs and their associated optics and electronics are usually bulky as well as expensive. Hence, they tend to be located in dedicated facilities and not moved from there. However, we understand that there are some field models in the market. LDVs are non-intrusive, a big advantage over other measuring devices that may disturb the very flow they are measuring. The laser beam has to cross the walls of the container as perpendicularly as possible to avoid velocity measurement errors and bias owing to differences in the refraction of the beam. When the measurements are to be done in a cylindrical container, it is best to build an outer container with a flat surface (preferably of high quality metacrilate plastic) and fill the jacket space with the same fluid that is to be measured. This way, the inner cylinder wall becomes transparent to the beam and it is much easier to align the beam perpendicularly to the outer flat surface.

Sometimes, natural suspended particles in the water can act as seeds. Generally, the fluid is seeded with artificial particles. In order for natural or artificial particles to be good tracers of the flow, they should be neutrally buoyant and small to minimize inertial effects. There is no impediment, in principle, to move the probe during data sampling so that the LDV can be used, for instance, in flow systems with zero average velocity. However, because of the sensitivity of the LDV and the nature of the measurements one needs a highly precise, vibration-free, positioning system, that would probably be more expensive than the LDV itself. When the fluctuating component of velocity is larger than the mean flow, and the sampling of flow velocity data is continuous, the analysis of time series data will give overestimates of kinetic energy and of dissipation, simply because there is a greater chance for fast moving particles to be found in the sampling volume. There are some sampling and data analysis solutions to this problem.

In non-zero mean flows, one can apply the equations of sections *Basic estimates of* ε or *Spectral analysis* to estimate ε. In set-ups where turbulence is generated by oscillating grids of large strokes, the estimation of ε is more challenging, since these equations cannot be applied. Moreover, a measure-

ment of turbulent diffusion away from the turbulence source is not applicable either, for the turbulence source is not fixed in space. Peters and Gross (1994) and Peters *et al.* (1996) made an approximation for such a system, by calculating turbulent kinetic energy (q) and applying Eq. 30 after assuming that the terms T, P, and B are all zero. As a kinetic energy term

$$q = \frac{1}{2}\mathbf{u}'^2 \tag{37}$$

Since $\mathbf{u}'$ is a vector, its modulus is

$$\sqrt{\left(u_x'^2 + u_y'^2 + u'^2\right)}.$$

The average q for the flow will be

$$q = \frac{1}{2}\left(\sigma_{u_x}^2 + \sigma_{u_y}^2 + \sigma_u^2\right) \tag{38}$$

where σ_u is the standard deviation of velocity in each spatial direction. Before applying Eq. 37, Peters and collaborators had to split the velocity time-series from a fixed point in space according to grid-oscillation frequency and superimposed all the sections. From the ensemble standard deviation they calculated the turbulent kinetic energy (q) at each point of the oscillating period. See Figure 9 for an example and a profile of measurements. ε was calculated from the decay of q over time, after the passage of the grid, $\varepsilon = dq/dt$. This decay was not constant in their system and hence they had a range of ε, the highest values again just after the grid passage and the smallest values just before the grid would come through again (Peters and Gross, 1994; Peters *et al.*, 1996). Saiz and Kiorboe (1995) applied a very similar mathematical approach using particle velocities obtained through videocinematography in a grid-generated turbulence set up.

Acoustic Doppler Velocimetry

Acoustic Doppler velocimeters (ADVs) are also available on the market nowadays. Their operating principle is identical to that of LDVs but instead of using an electromagnetic wave they use a sound wave. Commercial probes can be as small as ca. 5 cm in diameter and can provide 3-dimensional velocity information. They sample the three

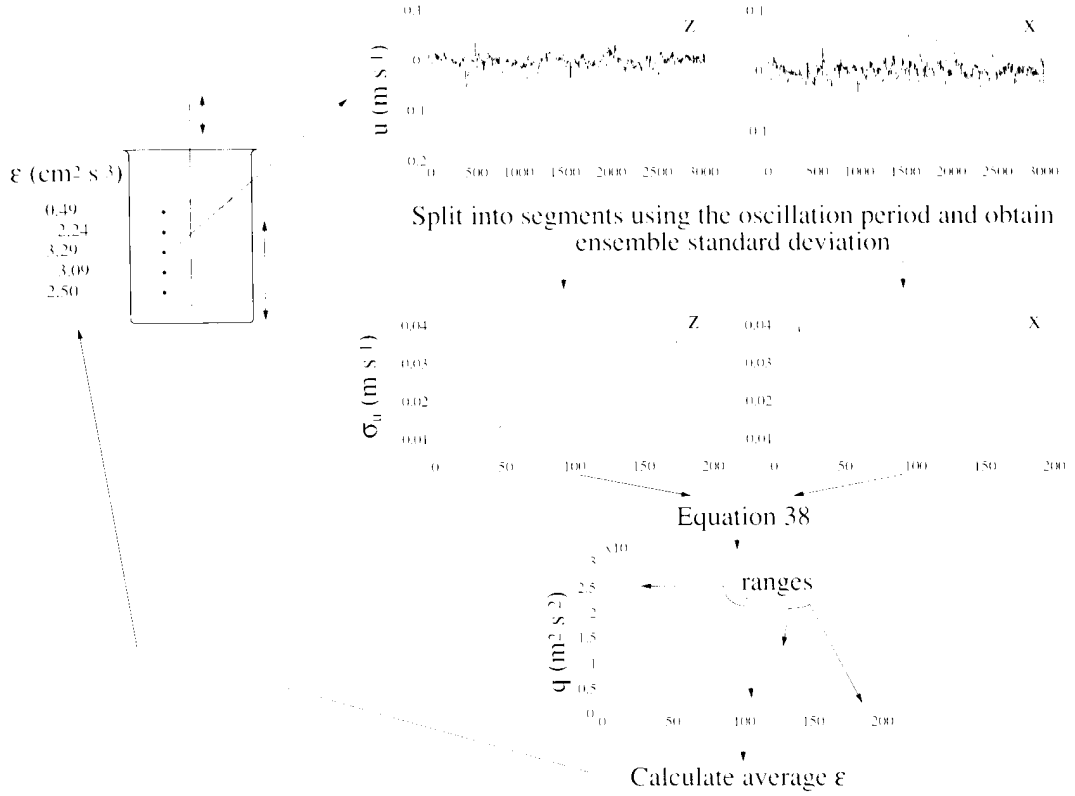

FIG. 9. Measurement of ε in a particular grid-generated turbulence system with a large stroke. The oscillation was of 31.5 rpm, sampling frequency was 100 Hz, x-axis of velocity plots show the first 3000 samples, x-axis of the other plots show time (s) once divided by 100. Velocity data was obtained using an TSI laser Doppler velocimeter. Data from Peters and Gross (1994).

velocity components of a relatively small common sampling volume (0.1 to 1 cm^3) at a distance of about 5 cm. Sampling rates of 25 Hz are available with short-term velocity errors of the order 1-10 mm s^{-1}. There are also fully submersible field probes available.

Compared to the LDV, the sampling volume is larger, and consequently the spatial resolution is smaller. Also, the probe is intrusive and has to be submerged in the fluid, which may not always be compatible with the experimental setup and may interfere with the flow being measured. But undoubtedly, acoustic Doppler velocimeters are much easier to use, maintain and move from one lab to the other or to field sites. An ADV was used by MacKenzie and Kiørboe (1995) to measure grid generated turbulence in their experimental containers, and it surely will be used more extensively in plankton studies both because of its ease of use and its low price compared to laser based systems.

Imaging techniques

A convenient way to investigate turbulent flow is by means of image analysis techniques. These techniques are based on the actual visualization of the flow and the analysis of the change in time of its structures. Some of the most appealing characteristics of these techniques are that 1) they allow the researcher to actually see the flow and directly study the dynamics of the spatially coherent structures, 2) fields of flow velocity can be measured in space instead of just measuring velocity at a single point, and 3) a range of scales of flow and their interactions can be seen simultaneously which is very important in the study of turbulence. Some of the constraints include having to generally view and analyze flow in two dimensions and then extrapolate to three dimensions, a trade-off between the area viewed and the smallest scales of turbulence that can be measured, a limit to measure small scales set by optics, the techniques' time consumption being very large compared to other methods, and sometimes the sheer hardware and software computing power needed to analyze the data.

The movement of water cannot be viewed directly, but first needs to be contrasted with some kind of tracer. The most widely used tracer is ink, which is adequate to follow mean flows but it is more tricky for measuring turbulence. Turbulence tends to homogenize the distribution of scalars, at least down to a certain scale, causing the water to lose its contrast. For biological experiments, if one needs to measure turbulence in enclosures which contain organisms, ink is inappropriate because of its toxicity to organisms and the difficulty in accurately measuring fluctuating flow velocities and direction. Below follow some flow visualization techniques in somewhat more detail.

Shadowgraph

An indirect method to measure small scale motion is to use either shadowgraph or Schliering, which detects density changes through changes in the refractive index. The fluid has to be stratified. Strickler and collaborators have gathered a wealth of information on planktonic crustacean movement using ever more refined optics (Strickler, 1977; Hwang *et al.*, 1994). With this system, they visualize the hydrodynamic effects that the movement of these organisms produce upon the water, and visualize swimming behavior and calculate energetic swimming costs. It should be possible to calculate turbulent energy dissipation from Schlieren images, by estimating the local velocities from spatial correlations of the moving shadows. This has not been done in relation to experiments with plankton, because turbulence would break up the density stratification that is needed to visualize the effect of the organisms on the fluid.

Particle tracking

When adding particles to a fluid we can track and record the movement of these particles by means of a photographic, video or CCD camera. This is a non-intrusive system and, in that sense, while measuring we are not disturbing the flow. The assumption here is that particles (5 to 100 μm in diameter for use in liquids) will perfectly follow streamlines and that by tracking the paths of particles we are visualizing the fluid flow. For this assumption to hold, particles have to be small and neutrally buoyant. As far as size goes, there is a tradeoff since the optics of our system have to be able to see the particles. The video recording will let us calculate the displacement of particles frame by frame and thus calculate velocities in two directions. It is much more difficult to obtain data for the third direction since it entails recording and analyzing the same particles with two orthogonally positioned cameras. The assumption is that the third dimension will be equal to one of the other two. With the data on particle velocities one

can then calculate the mean velocity and the fluctuating component of velocity for each particle and direction.

From this point one can apply energy dissipation estimates using the approach of sections *Basic estimates of* ε or *Spectral analysis* (Saiz, 1994). Using a different approach, turbulent diffusion can be calculated from the fluctuating component of velocity. This approach was used by Marrasé *et al.* (1990) in a system with a point source of turbulent energy at the top of their experimental unit. They videotaped particles at different distances from that source. They calculated the vertical turbulent diffusion at these distances as:

$$VTD_z = \frac{1}{2}\left(u'u_z'^2 + u'u_z'^2 + u'u'^2\right) \qquad (39)$$

where VTD_z is the vertical turbulent diffusion, and energy dissipation rates were calculated as:

$$\varepsilon = -\frac{\mathrm{d}VTD}{\mathrm{d}z} \qquad (40)$$

When a sufficient number of particles can be seen in each frame, one can actually reconstruct a flow velocity field. One subdivides the viewing area into a relevant scale uniform grid and has a velocity vector calculated in each subarea. To do so, there are techniques that interpolate velocities to fill in areas that didn't have particles, and alternatively, techniques that average velocities and directions in areas with many particles. For more information the paper by Stamhuis and Videler (1995) is a good starting point.

Sampling frequency should not be a problem from the recording mechanism point of view (professional U-matic video records at 50 frames per second, and high speed video or photography can do much better). The position of particles can be marked on a transparent plastic or paper sheet placed in front of the monitor. The video is played frame by frame and the track of particles is marked. When finished the points on the transparency are digitized, usually with a digitizing tablet and converted to actual distances to an origin applying an appropriate calibration scale. Since we know the time step between frames velocity time series for the particles can be calculated. The whole process can now be automated with appropriate hardware and software.

As one can see, this technique is extremely time consuming and can not be used for routine and quick measurements if one is analyzing long (in time) particle paths. The workload can be somewhat alleviated by marking particle positions less frequently, for instance only every 0.1 s provided this frequency satisfies our turbulence calculation needs. One can also generate digital movies, either from a videotape or directly from the camera, and then use some image analysis software to track the particles automatically over time or to mark the positions of the particles on the computer screen with the mouse. In any case, one needs a good digitizing card, a large amount of RAM, and if the digital movies have to be saved, a storage device such as a tape or a writable CD-ROM. To give an idea of computer needs, a digital movie of 150 frames (383 x 287 pixels, 256 grays) requires about 16 MB of RAM for the digitizing program only (NIH Image 1.60 running on a PowerPC 601 processor). If the movie is to be saved it will take about 8 MB of space after compression. Particle tracking can be performed fully automatically by dedicated programs such as DigImage (Dalziel, 1992, see also Adrian, 1991). Figure 10 shows an example of flow analyzed using particle tracking.

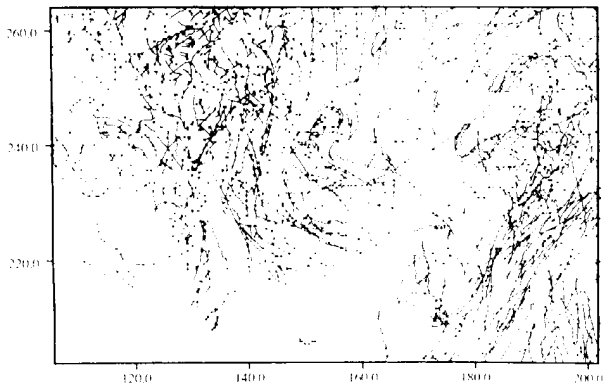

FIG. 10. – Example of particle tracking within a turbulent flow. The axes are in units of length (mm).

Particle Image Velocimetry

To observe the flow, the fluid is seeded with small particles to obtain sufficient scattered light. The fluid is illuminated by a light source. Often a laser beam is used for this purpose, but also a flash can be used in many cases. For two dimensional flow analyses (which is mostly the case) the light is deformed into a plane sheet by projecting the beam on a cylindrical lens or by projecting on a rotating mirror. The seeding particles that are illuminated by

the light sheet are imaged on a plane by a focal lens and recorded. Subsequent recordings of the illuminated particles result in particle traces that represent the local displacement of the fluid between illuminations. The subsequent illuminations might be recorded individually or on a single recording. At least two illuminations are needed for a PIV analysis, but three to five illuminations per analysis are often used to improve signal detectability.

If detailed information of the flow is needed, which is often the case for turbulent flows, the particle concentration must be high enough so that the spatial distances between the particles are smaller than the smallest spatial scale of the flow. An initial guess of the Kolmogorov micro-scale is a good measure for this.

For such high particle densities the individual particles between subsequent illuminations can not be recognized and therefore the particle displacements must be analyzed by means of statistical data analysis techniques. Therefore, the image is subdivided into small areas called interrogation regions. Within each interrogation region the mean displacement of the particles is calculated by estimating the autocorrelation function. This can be done in an optical or a digital way. For digital PIV the image is scanned in a computer. The correlation function of the gray values of the image pixels within an interrogation region are calculated by means of FFT. The first shifted peak of the correlation function then denotes the mean displacement between subsequent illuminations. Dividing the mean displacement by the time results in the local velocity. By analyzing all the interrogation regions, the entire flow pattern is obtained within the light sheet.

For a reliable analysis, the following points must be taken into account. 1) The signal detectability (expressed in signal to noise ratio) must be sufficiently high to detect a reliable estimation of the first shifted peak of the correlation function. At least four particle pairs must be present within the interrogation region. For a double exposed image the mean particle density must be 10 to 15 particles per interrogation region to obtain a reliability of 95%. 2) The particle displacement in the plane of the sheet between subsequent illuminations must be smaller than one-fourth of the interrogation region dimension and one fourth of the light sheet thickness in direction perpendicular to it. 3) The maximum of the first shifted peak can be estimated on sub-pixel level by interpolating the curve by a Gaussian function. The peak, therefore, must be recognized separately from the zero order peak. This means that a minimum particle displacement must be taken into account, which is about one particle diameter. A particle image must occupy at least three pixels for a curve fitting procedure. In that case the first-shifted peak can be estimated with a precision of 0.1 times the pixel diameter. 4) As particle pairs of small displacements are more frequent than those for large displacements, a bias results in the estimation direction to small displacements. Therefore, the velocity gradient within an interrogation region must be limited to 5%.

PIV has been used to analyze flow around a tethered copepod (Stamhuis and Videler, 1995) estimating velocity vector and vorticity fields among other parameters. A method similar to PIV, called speckle image velocimetry, is used when individual particles are indistinguishable. Then the correlation is applied to blobs within the fluid.

DISCUSSION

In this section we are not going to give a general discussion of the methods. We consider that all the methods and techniques mentioned in this review have been useful or may be useful in the future to generate and measure turbulence for studies with plankton. It will depend on the particular objectives of the study to decide which methods to use. Furthermore, new setups and measurement techniques are surely being developed as we write. What we will do is touch on some topics that may be important to consider in this interdisciplinary field.

Homogeneity

When doing biological experiments in a hydrodynamic setting we have to consider whether our conditions are homogeneous or not. If, for instance, we are trying to assess the effects of turbulence on a population of aquatic organisms and our experimental container presents a range of turbulence intensities, the results will be harder to interpret, since not all the organisms are going to experience the same levels of turbulence. Taking a more classical environmental variable, such as temperature, we should try to maintain the temperature constant and homogeneous for each experiment. On the other hand, the inhomogeneities in the turbulence intensity field can serve other purposes. If we can measure these inhomogeneities and they are constant in time, we could

identify the turbulence levels that motile organisms prefer by looking at the distribution of organisms in the container. Also, if we have a directional gradient of turbulence intensities and we are able to restrict organisms to a particular level, we could test an array of turbulence levels in a single experiment, which always reduces the experimental error. In any case, the question of turbulence homogeneity should be taken into account when designing experiments and when interpreting data.

Settling of organisms

Non-motile organisms in still water will settle as a function of their size and the difference of their density with that of water, with a terminal settling velocity derived from Stokes' law:

$$U_{settle} = \frac{2}{9} r_p g \frac{(\rho_p - \rho_w)}{\mu} \qquad (41)$$

where ρ is the buoyant density, r is the radius, and μ is the dynamic viscosity. The subindices indicate particle (p) and water (w). Settling speeds in turbulent flows can be different than in still water, but there is no unique law for the different particle sizes and the different levels of intensity (Jiahua, 1980).

In biological experiments settling can become a serious problem. The dynamics of growth and nutrient uptake for example may be very different depending on whether the organisms are close to an interface or free in the water. The homogeneity of the spatial distribution of particles, often a critical assumption while sampling and modeling, is broken. Settling is normally avoided by keeping the organisms resuspended through air bubbling, rotary shaking, or other means. But, these solutions also introduce turbulence and, unless one is interested in the mechanisms that keep cells suspended, they are not suitable if turbulence is our variable of interest. One way to have still water controls is to use experimental containers on a slow moving (less than ca. 1 rpm) Ferris wheel. The containers must be overfilled and tightly closed without air bubbles. Since the bottles are rotating, the particles are not experiencing a constant gravitational field, and do not settle. Of course, one can not sample the containers at different time intervals without refilling them, since air in the containers would break the stillness.

When working with particles that we know do not settle significantly over the time course of our experiment, we still have to make sure that our turbulence treatment is not affecting the settling rate. Peters and Gross (1994) tested that turbulence was not affecting the distribution of bacteria and flagellates, at least for the time of their incubation, by comparing the concentration of particles in the center of their experimental container before and after thoroughly mixing the water in the container. Had the distribution of organisms been affected by their turbulence treatment the concentrations would have been different. Of course, it could be of interest to study how different turbulence treatments could affect the distribution of particles suspended in water. Again, such issues have to be considered when planning experiments.

Couette cylinders

These devices have been very popular in experiments with plankton. Their popularity stems from the fact that, under appropriate dimensions and settings, they will present a constant laminar flow for which velocities and shear values are totally determined and do not require measurement. Based on the fact that, in nature, planktonic organisms are generally smaller than the Kolmogorov length scale and, thus hypothesized to be affected only by the remaining laminar shear field, experiments in Couette cylinders have been often equated to experiments under small-scale turbulence. The calculation of an energy dissipation term (Eq. 23), that can be compared to those obtained for small-scale turbulence has helped to establish this view.

Some researchers have taken care to limit the angular velocities to remain under pure Couette flow (Shimeta *et al.*, 1995). Others have viewed the type of flow using dye to distinguish whether they were generating laminar or turbulent flow (Mead and Denny, 1995). On the other hand, some Couette devices used in biology have been poorly designed, leaving 30% or more of their volume in the bottom wedge, certainly ensuring more instabilities than originally desired and probably presenting turbulent flow. This is aggravated because many planktonic organisms will settle during an experiment owing to gravity, collecting in the bottom of the Couette cylinder, and not being exposed to the type of flow defined between the two cylinder plates. Paradoxically, then, experiments done in Couette cylinders to test the effects of a laminar shear field on planktonic organisms often turn into tests of small-scale turbulence. These problems should be definitely taken into account when designing experiments.

Laboratory generated turbulence

Our aim is to reproduce turbulence representative of natural systems in a laboratory. The essential characteristic to be reproduced is turbulence intensity as expressed by turbulent energy dissipation rates, ε. Larger ε result in smaller space and time microscales (Table 1).

Viscosity of 36 psu seawater has a value around 0.01 $cm^2\ s^{-1}$ at 20°C (0.018 $cm^2\ s^{-1}$ at 0°C to 0.008 $cm^2\ s^{-1}$ at 30°C). Energy dissipation rate in the upper ocean ranges from about 5×10^{-7} to 5 $cm^2\ s^{-3}$ with a mean of 10^{-3} $cm^2\ s^{-3}$ (MacKenzie and Leggett, 1993). Applying Eq. 2, eddy motion exists down to a size scale of 0.02 cm to 2 cm, depending on energetic conditions. However, the Kolmogorov scale is not a precise cut-off between a range where eddies exist and a range where they do not. Hill *et al.* (1992) experimentally found that the movement of particles of sizes similar to the Kolmogorov microscale is dominated by eddying motion rather than viscous forces, and that turbulent eddy motion continues down to 1/6 λ_K. The Kolmogorov microscale is an approximation for the scale where viscous forces start to become important. For mathematical convenience, λ_K is often calculated as multiplied by 2π.

Turbulence levels used in experiments with plankton have been on average several orders of magnitude higher than levels in the ocean (Fig. 4), making it difficult to extrapolate results to natural systems. It is not so much that biologists prefer high turbulence than it is difficult to achieve low turbulence levels in the laboratory. In order to have dynamical similarity between the large scale ocean flows and the small scale laboratory experiments, the local Reynolds number should have the same value.

$$\mathrm{Re} = \frac{u' l}{\nu} = \text{const.} \qquad (42)$$

Since the integral scales, l, in the ocean are larger than in the experiments, the larger velocities needed to compensate the small scales in the laboratory, result in much higher dissipations. It is also true that the scales of energy input and the scales of energy dissipation are closer together in the laboratory, especially in small containers, than in the ocean. If these scales are too close, the full developement of an inertial subrange is hindered. Since most estimates of ε are based on the assumption of having an inertial subrange, many of the laboratory estimates could be wrong (Osborn, 1996).

Dissipation measurements in the ocean may be somewhat biased and underestimated. Probably higher dissipation rates are not uncommon in the upper 10 m since actual measurements are hindered by bad meteorological conditions. Even under calm conditions there are not that many physical measurements of small-scale turbulence, mostly because all measurements are done onboard ships which are subject to motions much greater than the dissipation scales. Sampling of the ship wake and the distance needed (about 10 m) for free-falling probes to reach terminal velocity (where measurements are reliable) are additional complications. Moreover, ε values tend to be averages. Intermittence of turbulence, coupled with interactions of surface and internal waves with the stratified density profile and fossil turbulence density microstructure, can give local dissipation rates several orders of magnitude larger than values averaged over time and space (Gibson, 1986; Baker and Gibson, 1987; Gibson, 1987; Gargett, 1989). This would help to bring together the plots in Figure 4 considerably.

CONCLUSIONS

It is critically important to be able to compare turbulence in the ocean with turbulence created in our experiments to extrapolate biological results to natural conditions. There still is considerable uncertainty about the levels of turbulence that planktonic organisms face in nature, and on the frequency and duration of a given level of turbulence. The intermittency of turbulence intensity is especially important to biology since the synchronization of biological phenomena depends on it. The same physical parameters when measured in the laboratory may bear an even greater uncertainty, mainly because of the difficulty to scale ocean to laboratory dynamics. If we could make use of changing viscosity, as in purely physical experiments, the scaling problem could probably be solved, but fish larva will not do well in honey, ethanol or air. Before these uncertainties are solved our experiments with plankton should be considered basically qualitative.

The choice of method to generate turbulence in the laboratory is not arbitrary and should depend on the biological questions being asked as well as on the feasibility of doing accurate measurements of turbulence in the experimetal containers. We have tried to describe advantages and disadvantages of

each of the methods to generate and measure turbulence in the laboratory. Perhaps those measurement techniques involving visualization have the brightest future since they offer spatial as well as temporal information. This will be especially true when, owing to the lack of a developed inertial subrange, we can not rely fully on spectral analysis. Optics and hardware will eventually improve to make visualization and analysis of flow fields in large areas with high resolution down to micrometer particles, and 3-dimensions a reality. To achieve these advancements promptly, active research and development in this field is greatly needed and encouraged.

APPENDIX

Since one needs to compare the turbulence used in the laboratory for experiments with plankton to the turbulence in the ocean, most of us will want to go out to sea and do measurements in our area of study. In this section we show several equations to estimate energy dissipation and turbulent viscosity other than the ones already seen above. They are chiefly used for measurements in the ocean but can be used in the laboratory taking into account the approximations and assumptions involved.

Most equations have the underlining assumption of homogeneous stationary turbulence with a large enough inertial subrange. If this assumption is met, the 3-D energy spectrum obeys the following equation

$$\frac{\partial E(k)}{\partial t} = T(k) - 2\nu k^2 E(k) \tag{43}$$

where here T indicates the transport of energy from one wavelength k to another with the overall limitation that

$$\int_0^\infty T(k)\,dk = 0 \tag{44}$$

There are several spectral models, which attempt to model Eq. 43. Notice that the last term, integrated over all wavelengths, is the turbulent dissipation ε. The difficulties involved in calculating ε from equation Eq. 43 or from Eq. 36 based on velocity spectra, are similar to those involved using Eq. 32 directly. Two velocity probes are needed in order to calculate the correlations in Eq. 35 or the velocity gradients in Eq. 32. The last resort is to use dimensional arguments as in Eq. 33 to find reasonable estimates. As the ocean is stratified, turbulent viscosity ν_T, depends on Brunt-Väisällä frequency N, and dissipation, as a measure of the turbulent energy:

$$\nu_T = 0.25\,\varepsilon N^{-2} \tag{45}$$

given by Denman and Gargett (1983). There are many such expressions relating dissipation to more readily measured parameters, both in deep waters and near the coast, but a great deal of caution must be taken when applying them to general situations. For example MacKenzie and Leggett (1993) derived an empirical relationship between the wind speed U and the dissipation profiles with depth:

$$\log \varepsilon(z) = \log U^{2.69} + \log z^{-1.32} - 4.812 \tag{46}$$

A similar relationship was given by Oakey and Elliott (1982) as

$$\varepsilon = \left(U^{0.91}\right)^{3/2} \tag{47}$$

Taking into account the drag coefficient between the wind and the water, Cd, their densities and the von Kármán constant κ, the following relationship is often used

$$\varepsilon = \left(\frac{\rho_{air}}{\rho_{water}} Cd\right)^{3/2} \frac{U^3}{\kappa z} \tag{48}$$

For more details, see MacKenzie and Leggett (1993), where other such empirical dissipation profiles are compared. One has to be aware that the energy production mechanisms are totally different in the bulk of a stratified region where internal wave breaking is the turbulent energy source and in a wind or wave stirred coastal region.

A quantity related to ε is eddy diffusivity or eddy viscosity, introduced by Boussinesq as a proportionality coefficient between the fluxes and the gradients, defined as

$$\nu_{T_{ij}} = \frac{\overline{u_i' u_j'}}{\dfrac{\partial U_i}{\partial x_j}} \tag{49}$$

$$k_{T_i} = \frac{\overline{u_i T}}{\dfrac{\partial T}{\partial x_i}} \tag{50}$$

for momentum and heat transport (Redondo, 1987).

Three basic models are used to calculate ν_T, in terms of the number and type of additional equations

needed. 1) With a single algebraic equation in terms of the integral length scale. These are called mixing length models

$$\nu_T = c\, l^2 \left| \frac{\partial u_i}{\partial x_j} + \frac{\partial u_j}{\partial x_i} \right| \tag{51}$$

2) Solving an equation for evolution of the turbulent kinetic energy q, such as the one given in Eq. 30, and using

$$\nu_t = c\, q^{1/2} l \tag{52}$$

3) Solving two equations, one for q and one for ε (q-ε or k-ε models), allows the use of the following relationship relating turbulent viscosity and dissipation

$$\nu_t = c \frac{q^2}{\varepsilon} \tag{53}$$

The constants c, are of order unity, but have to be experimentally calibrated. Also, in terms of dimensional arguments, the dissipation may be estimated from the turbulent kinetic energy and the integral length scale as

$$\varepsilon = c' q^{3/2} l^{-1} \tag{54}$$

with c' another constant. Then we also have

$$\nu_t = c'' q^{1/2} l \tag{55}$$

with the constants related as $c'=c''c$.

As stated above, it is not easy to measure velocity gradients, or even the value of the kinetic energy of the turbulence. Hence, temperature gradients are often measured and the rate of dissipation of temperature fluctuations measured as

$$\chi = 2k \overline{\nabla T' \nabla T'} \tag{56}$$

which behaves in a similar way as ε. The Cox number, which is often used in oceanography as

$$C_x = 3 \frac{\overline{\frac{\partial T'}{\partial t} \frac{\partial T'}{\partial t}}}{\left(\frac{\partial T}{\partial z} \right)^2} \tag{57}$$

assuming that the vertical velocity fluctuations are reflected in temperature fluctuations may be related to (χ) as

$$C_x = \frac{1}{2} \chi k \frac{\partial T}{\partial z} \tag{58}$$

If we relate the Elison length scale, as the ratio of temperature r.m.s to the vertical temperature gradient, to the Ozmidov scale (Osborn, 1980)

$$L_o = \left(\frac{\varepsilon}{N^3} \right)^{1/2} \tag{59}$$

and use the above expressions, we can give an estimate of dissipation in terms of temperature (or density) profile measurements as

$$\varepsilon = \frac{\overline{T'^2} \chi^2 k^2 N^3}{4 C_x^2} \tag{60}$$

for a stratified region. As a check on the measurements, χ should have a lognormal distribution (Davis, 1996).

If the stirring is due to wave breaking, Svendsen and Putrevu (1994) give a review of several expressions for the horizontal and vertical eddy viscosity in terms of the depth, z, and distance to the shore, x. Using Eq. 53, the dissipation may be expressed as a function of the surface wave speed $\sqrt{g z}$

$$\left(\nu_t = 0.015 x \sqrt{g z} \right) \rightarrow \varepsilon = 6.2 \times 10^{-4} g^{3/2} z^{1/2} \tag{61}$$

$$\left(\nu_t = 0.01 z \sqrt{g z} \right) \rightarrow \varepsilon = 4.2 \times 10^{-4} \frac{(g z)^{3/2}}{x} \tag{62}$$

ACKNOWLEDGEMENTS

The participants of the EC-MAST course *Ocean Turbulence: a basic environmental property for plankton* provided the most stimulating discussions. Brian MacKenzie, Cèlia Marrasé, Enric Saiz and an anonymous reviewer greatly improved previous versions of this paper. Gerber van der Graaf kindly provided information on PIV. Eduard Quintana partly composed Fig. 1. Funding for this work was provided by a EU grant MAS3-CT95-0016. F.P. also acknowledges a Spanish Ministry of Education Postdoctoral Fellowship, and J.M.R. acknowledges CAICYT grant UE95-0016 and EU grant MAS2-CT93-0053.

REFERENCES

Adrian, R.J. – 1991. Particle-imaging techniques for experimental fluid mechanics. *Annu. Rev. Fluid Mech.*, 23: 261-304.

Alcaraz, M., E. Saiz, and A. Calbet. – 1994. Small-scale turbulence and zooplankton metabolism: effects of turbulence on heartbeat rates of planktonic crustaceans. *Limnol. Oceanogr.*, 39: 1465-1470.

Alcaraz, M., E. Saiz., C. Marrasé and D. Vaqué. – 1988. Effect of

turbulence on the development of phytoplankton biomass and copepod populations in marine microcosms. *Mar. Ecol. Prog. Ser.*, 49: 117-125.

Baker, M.A. and C.H. Gibson. – 1987. Sampling turbulence in the stratified ocean: statistical consequences of strong intermittency. *J. Phys. Oceanogr.*, 17: 1817-1836.

Batchelor, G.K. and S. Stewart. – 1950. Anisotropy of the spectrum of turbulence at small wave numbers. *Quart. J. Appl. Mech.*, 3: 1-8.

Batchelor, G.K. and A.A. Townsend. – 1948 a. Decay of isotropic turbulence in the final period. *Proc. R. Soc. Lond. A.*, 194: 527-546.

Batchelor, G.K. and A.A. Townsend. – 1948 b. Decay of isotropic turbulence in the initial period. *Proc. R. Soc. Lond. A*, 193: 539-566.

Berdalet, E. – 1992. Effects of turbulence on the marine dinoflagellate *Gymnodinium nelsonii*. *J. Phycol.*, 28: 267-272.

Bradshaw, P. – 1979. *Turbulence and its measurement*. Cambridge University Press, London.

Britter, R.E. – 1984. Diffusion and decay in stably-stratified turbulent flows. *In*: J.C.R. Hunt (ed.): *Turbulence and diffusion in stable environments*. Oxford Science Publications.

Britter, R.E., J.C.R. Hunt, G.L. Marsh and W.H.J. Snyder. – 1983. The effects of stable stratification on turbulent diffusion and the decay of grid turbulence. *J. Fluid Mech.*, 127: 27-44.

Charlson, R.J., J.E. Lovelock, M.O. Andreae and S.G. Warren. – 1987. Oceanic phytoplankton, atmospheric sulphur, cloud albedo and climate. *Nature*, 326: 655-661.

Clifford, N.J. and J.R. French. – 1993. Monitoring and modelling turbulent flow: historical and contemporary perspectives. *In*: N.J. Clifford, J.R. French and J. Hardisty (eds.): *Perspectives on flow and sediment transport*, pp. 1-34. John Wiley & Sons Ltd.

Costello, J.H., J. R. Strickler, C. Marrasé, G. Trager, R. Zeller and A.J. Freise. – 1990. Grazing in a turbulent environment: behavioral response of a calanoid copepod, *Centropages hamatus*. *Proc. Natl. Acad. Sci. USA.*, 87: 1648-1652.

Dalziel, S.B. – 1992. Decay of rotating turbulence: some particle tracking experiments. *Appl. Sci. Res.*, 49: 217-244.

Davis, R.E. – 1996. Sampling turbulent dissipation. *J. Phys. Oceanogr.*, 26: 341 358.

Denman, K.L. and A.E. Gargett. – 1983. Time and space scales of vertical mixing and advection of phytoplankton in the upper ocean. *Limnol. Oceanogr.*, 28: 801-815.

Dickey, T.D. and G.L. Mellor. – 1980. Decaying turbulence in neutral and stratified fluids. *J. Fluid. Mech.*, 99: 13-31.

Durst, F., B. Schonung, K. Selanger and M. Winter. – 1986. Bubble-driven liquid flows. *J. Fluid Mech.*, 170: 53-82.

Estrada, M., M. Alcaraz and C. Marrasé. – 1987. Effects of turbulence on the composition of phytoplankton assemblages in marine microcosms. *Mar. Ecol. Prog. Ser.*, 38: 267-281.

Fernando, H.J.S. – 1991. Turbulent mixing in stratified fluids. *Ann. Rev. Fluid Mech.* 23: 455-493.

Gallego, A., M.R. Heath, E. McKenzie and L.H. Cargill. – 1996. Environmentally induced short-term variability in the growth rates of larval herring. *Mar. Ecol. Prog. Ser.*, 137: 11-23.

Gargett, A. – 1989. Ocean turbulence. *Ann. Rev. Fluid. Mech.*, 21: 419-451.

Gargett, A. – 1997. "Theories" and techniques for observing turbulence in the ocean euphotic zone. *Sci. Mar.* (this volume).

Gibson, C.H. – 1986. Internal waves, fossil turbulence and composite ocean microstructure spectra. *J. Fluid Mech.*, 168: 89-117.

Gibson, C.H. – 1987. Fossil turbulence and intermittency in sampling oceanic mixing processes. *J. Geophys. Res.*, 92: 5383-5404.

Gibson, C.H. and W.H. Thomas. – 1995. Effects of turbulence on growth inhibition of a red tide dinoflagellate, *Gonyaulax polyedra* Stein. *J. Geophys. Res.*, 100: 24841-21846.

Giesy, Jr., J.P. (ed.) -1980. *Microcosms in ecological research*. U.S. Department of Energy.

Hannoun, I.A. and E.J. List. – 1988. Turbulent mixing at a shear-free density interface. *J. Fluid Mech.*, 189: 211-234.

Hellung-Larsen, P. and I. Lyhne. – 1992. Effect of shaking on the growth of diluted cultures of *Tetrahymena*. *J. Protozool.*, 39: 345-349.

Hill, P.S., A.R.M. Nowell and P.A. Jumars. Encounter rate by turbulent shear of particles similar in diameter to the Kolmogorov scale. *J. Mar. Res.*, 50: 643-668.

Hopfinger, E.J. – 1987. Turbulence collapse in stratified fluids. IUTAM symposium on mixing in stratified fluids. Margaret river, Western Australia. *J. Geophys. Res.*, 92: 5248-.

Hopfinger, E.J. and J.A. Toly. – 1976. Spatially decaying turbulence and its relation to mixing across density interfaces. *J.Fluid Mech.*, 78: 175-188.

Howarth, R.W., T. Butler, K. Lunde, D. Swaney and C.H. Chu. – 1993. Turbulence and planktonic nitrogen fixation: a mesocosm experiment. *Limnol. Oceanogr.*, 38: 1696-1711.

Hwang, J.-S., J.H. Costello and J.R. Strickler. – 1994. Copepod grazing in turbulent flow: elevated foraging behavior and habituation of escape responses. *J. Plankton Res.*, 16: 421-431.

Jenkinson, I.R. – 1993. Viscosity and elasticity of *Gyrodinium* cf. *aureolum* and *Noctiluca scintillans* exudates, in relation to mortality of fish and damping of turbulence. *In*: T.J. Smayda and Y. Shimizu (eds.): *Toxic phytoplankton blooms in the sea*, pp. 757-762. Elsevier, Amsterdam.

Jiahua, F. – 1980. Experimental studies on the diffusion of sediment particles in turbulent fluid. *Scientia Sinica*, 1: 99-112.

LaBarbera, M. and S. Vogel. – 1976. An inexpensive thermistor flowmeter for aquatic biology. *Limnol. Oceanogr.*, 21: 750-756.

Landry, E., T.J. Miller and W.C. Leggett. – 1995. The effects of small-scale turbulence on the ingestion rate of fathead minnow (*Pimephales promelas*) larvae. *Can. J. Fish. Aquat. Sci.*, 52: 1714-1719.

Launder, B.E. and D.B. Landry. – 1972. *Mathematical models of turbulence*. Academic Press, London.

Lazier, J.R.N. and K.H. Mann. – 1989. Turbulence and the diffusive layers around small organisms. *Deep Sea Res.*, 36: 1721 1733.

Legendre, L., S. Demers and D. LeFaivre. – 1986. Biological production at marine ergoclines. *In*: J.C.J. Nihoul (ed.): *Marine Interfaces Ecohydrodynamics*, pp. 1-54. Elsevier, Amsterdam.

Lin, J.T. and Y.H. Pao. – 1979. Wakes in stratified fluids. *Ann. Rev. Fluid Mech.*, 11: 317-338.

Linden, P.F. – 1979. Mixing in stratified fluids. *Geophys. Astrophys. Fluid Dyn.*, 13: 3-23.

Linden, P.F. – 1980. Mixing across a density interfaces produced by grid turbulence. *J. Fluid Mech.*, 100: 691 703.

MacKenzie, B.R. and T. Kiorboe. – 1995. Encounter rates and swimming behaviour of pause-travel and cruise larval fish predators in calm and turbulent laboratory environments. *Limnol. Oceanogr.*, 40: 1278-1289.

MacKenzie B.R. and W.C. Leggett. – 1993. Wind-based models for estimating the dissipation rates of turbulent energy in aquatic environments: empirical comparisons. *Mar. Ecol. Prog. Ser.*, 94: 207-216.

Maillet, G.L. and D.M. Checkley, Jr. – 1991. Storm-related variation in the growth rate of otoliths of larval Atlantic menhaden *Brevoortia tyrannus*: a time series analysis of biological and physical variables and implications for larva growth and mortality. *Mar. Ecol. Prog. Ser.*, 79: 1-16.

Margalef, R. – 1978. Life-forms of phytoplankton as survival alternatives in an unstable environment. *Oceanologica Acta.*, 1: 493-509.

Margalef, R. – 1983. *Limnología*. Ediciones Omega, Barcelona.

Marrasé, C., J.H. Costello, T. Granata and J.R. Strickler. – 1990. Grazing in a turbulent environment: energy dissipation, encounter rates, and efficacy of feeding currents in *Centropages hamatus*. *Proc. Natl. Acad. Sci. USA.*, 87: 1653-1657.

McDougall, T.J. – 1979. Measurements of turbulence in a zero-mean-shear mixed layer. *J. Fluid. Mech.*, 94: 409

McEwan, A.D. – 1983. Internal mixing in stratified fluids. *J. Fluid Mech.*, 128: 59-80.

Mead, K.S. and M.W. Denny. – 1995. The effects of hydrodynamic shear stress on fertilization and early development of the purple sea urchin *Strongylocentrotus purpuratus*. *Biol. Bull.*, 188: 46-56.

Moeseneder, M.M. and G.J. Herndl. – 1995. Influence of turbulence on bacterial production in the sea. *Limnol. Oceanogr.*, 40: 1466-1473.

Monin, A.S. and R.V. Ozmidov. – 1985. *Turbulence in the ocean*. D. Reidel Publishing Company, Dordrecht, The Netherlands.

Moreira, J.L., P.M. Alves, J.G. Aunins and M.J.T. Carrondo. – 1995. Hydrodynamic effects on BHK cells grown as suspended natural assemblages. *Biotechnol. Bioeng.*, 46: 351-360.

Nixon, S.W., D. Alonso, M.E.Q. Pilson and B.A. Buckney. – 1980. Turbulent mixing in aquatic microcosms. *In*: J.P. Giesy Jr. (ed.): *Microcosms in ecological research*, pp. 818-849. U.S. Department of Energy.
Oakey, N.S. and J.A. Elliott. – 1982. Dissipation within the surface mixed layer. *J. Phys. Oceanogr.*, 12: 171-185.
Okubo, A. and R.V. Ozmidov. – 1970. Empirical dependence of the coefficient of horizontal turbulent diffusion in the ocean on the scale of the phenomena in question. *Izv. Atm. Ocean. Phys.*, 5: 308-309.
Osborn, T.R. – 1980. Estimates of the local rate of vertical diffusion from dissipation measurements. *J. Phys. Oceanogr.*, 10: 83-89.
Osborn, T.R. – 1996. The role of turbulent diffusion for copepods with feeding currents. *J. Plankton Res.*, 18: 185-195.
Ottersen, G. and S. Sundby. – 1995. Effects of temperature, wind and spawning stock biomass on recruitment of Arcto-Norwegian cod. *Fish. Oceanogr.*, 4: 278-292.
Peters, F. J.W. Choi and T. Gross. – 1996. *Paraphysomonas imperforata* (Protista, Chrysomonadida) under different turbulence levels: feeding, physiology and energetics. *Mar. Ecol. Prog. Ser.*, 134: 235-245.
Peters, F. and T. Gross. – 1994. Increased grazing rates of microplankton in response to small-scale turbulence. *Mar. Ecol. Prog. Ser.*, 115: 299-307.
Phillips, O.M. – 1977. *The dynamics of the upper ocean*. Cambridge University Press, London.
Pollingher, U. and E. Zemel, E. – 1981. In situ and experimental evidence of the influence of turbulence on cell division processes of *Peridinium cinctum* forma *westii* (Lemm.) Lefèvre. *Br. Phycol. J.*, 16: 281-287.
Powell, T.M. and A. Okubo. – 1994. Turbulence, diffusion and patchiness in the sea. *Phil. Trans. R. Soc. Lond. B.*, 343: 11-18.
Redondo, J.M. – 1987. *Difusión turbulenta en fluidos estartificados*. Ph. D. Thesis, Univ. Barcelona.
Redondo, J.M. – 1988. Difusión turbulenta por rejilla oscilante. Revista de Geofísica, 44: 163-174.
Redondo J.M. and P.F. Linden. – 1993. Mixing produced by Rayleigh-Taylor instabilities. In: S.D. Mobbs and J.C. King: *Waves and turbulence in stably stratified flows*. IMA 40: 395-422
Rothschild, B.J. (ed.). – 1988. *Toward a theory on biological-physical interactions in the world ocean*. Kluwer Academic Publishers, Dordrecht, The Netherlands.
Rouse, H. and J. Dodu. – 1955. Turbulent diffusion across a density discontinuity. *La Houille Blanche*, 10: 522-532.
Saiz, E. – 1994. Observations of the free-swimming behavior of *Acartia tonsa*: effects of food concentration and turbulent water motion. *Limnol. Oceanogr.*, 39: 1566-1578.
Saiz, E. and M. Alcaraz. – 1991. Effects of small-scale turbulence on development time and growth of *Acartia grani* (Copepoda: Calanoida). *J. Plankton Res.*, 13: 873-883.
Saiz, E. and M. Alcaraz. – 1992a. Enhanced excretion rates induced by small-scale turbulence in *Acartia* (Copepoda: Calanoida). *J. Plankton Res.*, 14:681-689.
Saiz, E. and M. Alcaraz. – 1992b. Free-swimming behaviour of *Acartia clausi* (Copepoda: Calanoida) under turbulent water movement. *Mar. Ecol. Prog. Ser.*, 80: 229-236.
Saiz, E., M. Alcaraz and G.-A. Paffenhöfer. – 1992. Effects of small-scale turbulence on feeding rate and gross-growth efficiency of three *Acartia* species (Copepoda: Calanoida). *J. Plankton Res.*, 14: 1085-1097.
Saiz, E. and T. Kiørboe. – 1995. Predatory and suspension feeding of the copepod *Acartia tonsa* in turbulent environments. *Mar. Ecol Prog. Ser.*, 122: 147-158.
Sathyendranath, S., A.D. Gouveia, S.R. Shetye, P. Ravindran and T. Platt. – 1991. Biological control of surface temperature in the Arabian Sea. *Nature*, 349: 54-56.
Savidge, G. – 1981. Studies of the effects of small-scale turbulence on phytoplankton. *J. Mar. Biol. Ass. U.K.*, 61: 477-488.
Schlichting, H. – 1987. *Boundary-layer theory*. McGraw-Hill, New York.
Shimeta, J., P.A. Jumars and E.J. Lessard. – 1995. Influences of turbulence on suspension feeding by planktonic protozoa: experiments in laminar shear fields. *Limnol. Oceanogr.*, 40: 845-859.
Stamhuis, E.J., and J.J. Videler. – 1995. Quantitative flow analysis around aquatic animals using laser sheet particle image velocimetry. *J. exp. Biol.*, 198: 283-294.
Stillinger, D.C., K.N. Helland and C.W. Van Atta. – 1983. Experiments on the transition of homogeneous turbulence to internal waves in a stratified fluid. *J. Fluid Mech.*, 131: 91-122.
Strickler, J.R. – 1977. Observation of swimming performances of planktonic copepods. *Limnol. Oceanogr.*, 22: 165-170.
Sundby, S. and P. Fossum. – 1990. Feeding conditions of Arcto-norwegian cod larvae compared with the Rothschild-Osborn theory on small-scale turbulence and plankton contact rates. *J. Plankton Res.*, 12: 1153-1162.
Svendsen, I.A. and Y. Putrevu. – 1994. Nearshore mixing and dispersion. *Proc. R. Soc. London A.*, 445: 561-576.
Tan, H.S. and S.C. Ling. – 1963. Final stage decay of grid-produced turbulence. *Phys. Fluids*, 6: 1693-1699.
Tennekes, H.H. and J.L. Lumley. – 1972. *A first course in turbulence*. MIT Press, Cambridge, MA.
Thomas, C.R., M. Al-Rubeai and Z. Zhang. – 1994. Prediction of mechanical damage to animal cells in turbulence. *Cytotechnology*, 15: 329-355.
Thomas, W.H. and C.H. Gibson. – 1990a. Effects of small-scale turbulence on microalgae. *J. App. Phycol.*, 2: 71-77.
Thomas, W.H. and C.H. Gibson. – 1990b. Quantified small-scale turbulence inhibits a red tide dinoflagellate, *Gonyaulax polyedra* Stein. *Deep-Sea Res.*, 37: 1583-1593.
Thomas, W.H. and C.H. Gibson. – 1992. Effects of quantified small-scale turbulence on the dinoflagellate *Gymnodinium sanguineum* (*splendens*): contrast with *Gonyaulax* (*Lingulodinium*) *polyedra*, and the fishery implication. *Deep-Sea Res.*, 39: 1429-1437.
Thomas, E.H., M. Vernet and C.H. Gibson. – 1995. Effects of small-scale turbulence on photosynthesis, pigmentation, cell division, and cell size in the marine dinoflagellate *Gonyaulax polyedra* (Dinophyceae). *J. Phycol.*, 31: 50-59.
Thomson, S.M. – 1969. *Turbulent interfaces generated by an oscillating grid in a stably stratified fluid*. Ph D. Thesis, Univ. Cambridge.
Thomson, S. M. and J.S. Turner. – 1975. Mixing across an interface due to turbulence generated by an oscillating grid. *J. Fluid Mech.*, 67: 349-368.
Toma, M.K., M.P. Ruklisha, J.J. Vanags, M.O. Zeltina, M.P. Leite, N.I. Galinina, U.E. Viesturs and R.P. Tengerdy. – 1991. Inhibition of microbial growth and metabolism by excess turbulence. *Biotechnol. and Bioeng.*, 38: 552-556.
Tritton, D.J. – 1988. *Physical fluid dynamics*. Clarendon Press, Oxford.
Turner, J.S. – 1968. The influence of molecular diffusivity on turbulent entrainment across a density interface. *J. Fluid Mech.*, 33: 639-656.
Turner, J.S. – 1973. *Buoyancy effects in fluids*. Cambridge University Press., London.
Vogel, S. – 1989. *Life in moving fluids*. Princeton University Press, Princeton, New Jersey.
White, A.W. – 1976. Growth inhibition caused by turbulence in the toxic marine dinoflagellate *Gonyaulax excavata*. *J. Fish. Res. Bd. Can.*, 33: 2598-2602.